IAEA
International Atomic Energy Agency

INDC(CPR)-062
Distr. NC

INDC International Nuclear Data Committee

Proceedings of the

Seventh AASPP Workshop on Asian Nuclear Reaction Database Development

China Institute of Atomic Energy, Beijing, China

8 – 11 November 2016

Edited by

Guochang Chen
China Institute of Atomic Energy, Beijing, China

and

Naohiko Otuka
Nuclear Data Section, International Atomic Energy Agency, Vienna, Austria

June 2017

IAEA Nuclear Data Section, Vienna International Centre, A-1400 Vienna, Austria

Selected INDC documents may be downloaded in electronic form from
http://www-nds.iaea.org/publications/
or sent as an e-mail attachment.
Requests for hardcopy or e-mail transmittal should be directed to
nds.contact-point@iaea.org
or to:

Nuclear Data Section
International Atomic Energy Agency
Vienna International Centre
PO Box 100
A-1400 Vienna
Austria

Produced by the IAEA in Austria
June 2017

INDC (CPR)-062
Distr. NC

Proceedings of the

Seventh AASPP Workshop on Asian Nuclear Reaction Database Development

China Institute of Atomic Energy, Beijing, China

8 – 11 November 2016

Edited by

Guochang Chen
Hokkaido University, Sapporo, Japan

and

Naohiko Otuka
Nuclear Data Section, International Atomic Energy Agency, Vienna, Austria

June 2017

Abstract

The 7th Workshop on Asian Nuclear Reaction Database Development was held from 8-11 November 2016 at China Hall of Science and Technology Hotel, Beijing, China. This 7th workshop followed the workshops in Sapporo (Japan, 2010), Beijing (China, 2011), Pohang (Korea, 2012), Almaty (Kazakhstan, 2013), Mumbai (India, 2014) and Sapporo (Japan, 2015). The workshop was coordinated by the Asian Centre Heads of the International Network of Nuclear Reaction Data Centres and supported by International Atomic Energy Agency. The topics of the workshop were sharing information on activities of the nuclear data centres, EXFOR compilation, data evaluation, computational simulations, software training and other related topics. The participants were attended from Austria, China, Japan, Kazakhstan, Korea and Mongolia. In the workshop, 18 presentations were presented and summarized in these proceedings.

Table of Contents

Agenda

Date	Time	Program	Participant	Chairman
Nov. 8 (Tue.)	9:30 -- 10:00	Registration		
	10:00 -- 11:00	Opening & Welcome Address		Zhigang Ge
	11:00 -- 11:30	Coffee Break & Group Photo		
	11:30 -- 12:30	EXFOR–status, compilation activities and new developments	V.Semkova (IAEA)	
	12:30 -- 14:00	Lunch		
	14:00 -- 14:50	Activation cross sections of alpha-induced reactions on natural palladium for ^{103}Ag production	M.Aikawa (Hokkaido University)	Xichao Ruan
	14:50 -- 15:40	Recently Progress of Nuclear Data Evaluations and Activities in China	Zhigang Ge (CIAE)	
	15:40 -- 16:10	Coffee Break		
	16:10 -- 16:40	Nuclear data measurement activities at CIAE	Xichao Ruan (CIAE)	M.Aikawa
	16:40 -- 17:10	Nuclear Data Activities using Cyclotron and electron linac	Kim Guinyun (Kyungpook National University)	

Date	Time	Program	Participant	Chairman
	18:00 -- 20:00	Welcome Banquet		
Nov. 9 (Wed.)	9:00 -- 9:50	Recent Nuclear Data Activities at KAERI	Young-Sik Cho (KAERI)	Kim Guinyun
	9:50 -- 10:40	An evaluation of alpha-clustering in (n, α) reaction and alpha-decay	Myagmarjav Odsuren (National University of Mongolia)	
	10:40 -- 11:00	Coffee Break		
	11:00 -- 11:30	Measurements and evaluations of excitation functions at CIAE	Jiang Liyang (CIAE)	Young-Sik Cho
	11:30 -- 12:00	Review of fission product yields measurements in key laboratory of nuclear data	Feng Jing (CIAE)	
	12:00 -- 14:00	Lunch		
	14:00 -- 14:30	Evaluation of deuteron-induced excitation functions for ^{186}W(d, p)^{187}W and ^{186}W(d, 2n)^{186}Re	Jimin Wang (CIAE)	Myagmarjav Odsuren
	14:30 -- 15:00	Low energy scattering cross sections for ^{6}Li+n and ^{7}Li+n reactions	Ichinkhorloo Dagvadorj (JCPRG)	
	15:00 -- 15:30	A new java-based EXFOR editor	Aiganym Sarsembayeva	

Date	Time	Program	Participant	Chairman
			(JCPRG)	
	15:00 -- 15:30	Coffee Break		
	15:30 -- 17:30	EXFOR Compilation	All	
Nov. 10 (Thu.)	9:00 -- 9:50	Investigation of Activation Cross-Sections of Alpha-Induced Nuclear Reactions on Natural Silver	Kim Kwangsoo (Kyungpook National University)	V.Semkova
	9:50 -- 10:40	Measurement and EXFOR Compilation of the Neutron-Induced Activation Cross Sections in the Energy Range up to 20 MeV	V.Semkova (IAEA)	
	10:40 -- 11:00	Coffee Break		
	11:00 -- 11:30	Recent EXFOR Compilation in CNDC	Guochang Chen (CIAE)	Zhigang Ge
	11:30 -- 12:00	Theoretical calculation of $n+^{6}Li$	Xi Tao (CIAE)	
	12:00 -- 14:00	Lunch		
	14:00 -- 14:50	Introduction of digitization software GDgraph	Guochang Chen (CIAE)	Zhigang Ge
	14:50 -- 15:50	GDgraph training		

Date	Time	Program	Participant	Chairman
	15:50 -- 16:20	Coffee Break		
	16:20 -- 17:30	EXFOR Compilation	All	
Nov. 11 (Fri.)	9:00 -- 10:00	Closing remarks		Zhigang Ge

EXFOR – Status, compilation activities and new developments

V. Semkova, N. Otuka and V. Zerkin

Nuclear Data Section, International Atomic Energy Agency, Vienna, Austria

The EXFOR database [1] is a global repository of experimental nuclear reaction data and associated information developed and maintained by the international collaboration of Nuclear Reaction Data Centres (NRDC) [2] under the auspices of the International Atomic Energy Agency Nuclear Data Section for data exchange since 1970. The high degree of coverage of all published experimental studies within the scope of EXFOR and the high quality of the compilations made the EXFOR library a valuable source for information and analysis.

The open literature (journals, conference proceedings, report etc.) is regularly scanned to identify publications reporting nuclear reaction data. In addition the EXFOR completeness is periodically checked and missing publications are compiled. The compilation of the articles in a timely manner and the efforts to minimise the time from the publication to the uploading of the EXFOR entry in database is important to provide up-to-date information to users.

Nuclear Data Section has recently organised Consultants' Meetings (CM) [3,4] in order to improve the EXFOR compilation for specific type of data and provide the necessary information for the proper analysis of the experimental data. Guidelines for compilation of the time-of-flight measurements and the thermal neutron scattering experiments were prepared and supplementary data (spectrometers' response function, phonon spectrum, structural parameters etc.) will be provided to users.

The status of the EXFOR compilation statistics and some new developments in the compilation of the experimental nuclear reaction data will be presented.

Reference

[1] N. Otuka et al., Nucl. Data Sheets, **120**, 272–276 (2014)

[2] International Network of Nuclear Reaction Data Centres www-nds.iaea.org/nrdc/

[3] CM on EXFOR Data in Resonance Region and Spectrometer Response Function, Report INDC(NDS)-0647, https://www-nds.iaea.org/index-meeting-crp/CM-RF-2013/

[4] CM on EXFOR Compilation of Thermal Neutron Scattering Data, Report INDC(NDS)-697, https://www-nds.iaea.org/index-meeting-crp/CM-THSC-2015/

Activation cross sections of alpha-induced reactions on natural palladium for ^{103}Ag production

M. Aikawa[1], M. Saito[1], Y. Komori[2], H. Haba[2], S. Takács[3], F. Ditrói[3], Z. Szűcs[3]

[1]*Graduate School of Science, Hokkaido University, Sapporo 060-0810, Japan*
[2]*Nishina Center for Accelerator-Based Science, RIKEN, Wako 351-0198, Japan*
[3]*Institute for Nuclear Research, Hungarian Academy of Sciences (ATOMKI), 4026 Debrecen, Hungary*

Production cross sections induced by neutrons and light charged-particles are fundamental information for applications of radioactive isotopes (RI). One such RI for medical applications is ^{103}Pd ($T_{1/2}$ = 16.991 d) for brachytherapy [1,2] and targeted radionuclide therapy as part of the ^{103}Pd/^{103m}Rh *in vivo* generator[3]. In addition to direct ^{103}Pd production, the production of its parent, ^{103}Ag, is worthy of investigation. ^{103}Ag has the isomeric state ^{103m}Ag at 134.4 keV ($T_{1/2}$ = 5.7 s, IT: 100%), which cumulatively contributes to the ground state ^{103g}Ag ($T_{1/2}$ = 65.7 min, $\varepsilon+\beta^+$: 100%) through the IT decay.

The ^{103}Pd isotope can be produced through the neutron capture (n, γ) reaction on ^{102}Pd in reactors [4,5]. However, the natural abundance of ^{102}Pd is only 1.02% [6] and its enrichment may be required for applications. In the case of alpha-induced reactions on ^{nat}Pd, experimental data are available only below 37 MeV [7]. Therefore, in this paper, we measured the excitation function of the ^{nat}Pd(α, x)^{103}Ag reaction up to 50.1 MeV.

The experiment was performed at the RIKEN AVF cyclotron by using the stacked foil technique and the activation method. ^{nat}Pd foils (purity: 99.95%, Nilaco, Japan) were used with ^{nat}Ti monitor foils (purity: 99.9%, Goodfellow, UK). The thicknesses of the Pd and Ti foils were estimated from measured area and weight of large foils and found to be 9.80 mg/cm^2 and 4.95 mg/cm^2, respectively. The stacked target consisted of 12 sets of the Pd-Pd-Ti-Ti foils (10 × 10 mm^2) cut off from the large foils. The pairs of the same elemental foils were stacked to compensate recoil losses of the products in every second foil at the downstream side of the beam. The target was irradiated for 2 hours by the 51.2-MeV alpha beam with the average intensity of 55.7 pnA, which was measured by a Faraday cup. The beam energy was measured by the time-of-flight method using a plastic scintillator monitor [8]. The γ-lines from the irradiated foils were measured by HPGe detectors.

The energy degradation of the beam in the stack was calculated using the polynomial approximation of the stopping power data [9]. The excitation function of the monitor ^{nat}Ti(α, x)^{51}Cr reaction was compared with the recommended cross

section data[10] and found in good agreement.

Table 1. Reaction and decay data of ^{103}Ag.

Residual	Half-life (min)	Decay mode (%)	E_γ (keV)	I_γ (%)	Contributing reactions	Q-value (keV)
^{103}Ag	65.7	EC (100)	118.74	31.2(20)	^{102}Pd(α, t)	-15655.6
					^{104}Pd(α, t2n)	-33808.29
					^{105}Pd(α, t3n)	-40356.32
					^{106}Pd(α, t4n)	-49917.29
					^{102}Pd(α, 3n)^{103}Cd(ε)	-29068.05

The reaction and decay data of ^{103}Ag ($T_{1/2}$ = 65.7 min) are shown in Table 1. The γ-line at 118.74 keV (31.2%) from the decay of ^{103}Ag was used to derive the excitation function of the ^{nat}Pd(α, x)^{103}Ag reaction. The ^{103}Ag isotope is also cumulatively produced from the decay of ^{103}Cd ($T_{1/2}$ = 7.3 min). The present result is shown in Fig. 1 together with the previous experimental data [7] and the TENDL-2015 data [10]. Our result confirmed the previous data below 37 MeV within the errors. The peak of the excitation function was found for the first time at around 42 MeV, which is consistent with the TENDL-2015 data.

In summary, we performed the experiment of the alpha-induced reactions on natural palladium to produce ^{103}Ag, which is a parent of ^{103}Pd available for brachytherapy. The excitation function of the ^{nat}Pd(α, x)^{103}Ag reaction was measured up to 50.1 MeV and found in consistent with previous experiment and theoretical calculation.

Acknowledgements

This work was performed at the RI Beam Factory operated by the RIKEN Nishina Center and CNS, University of Tokyo. This work is supported by the Japan - Hungary Research Cooperative Program, JSPS and HAS.

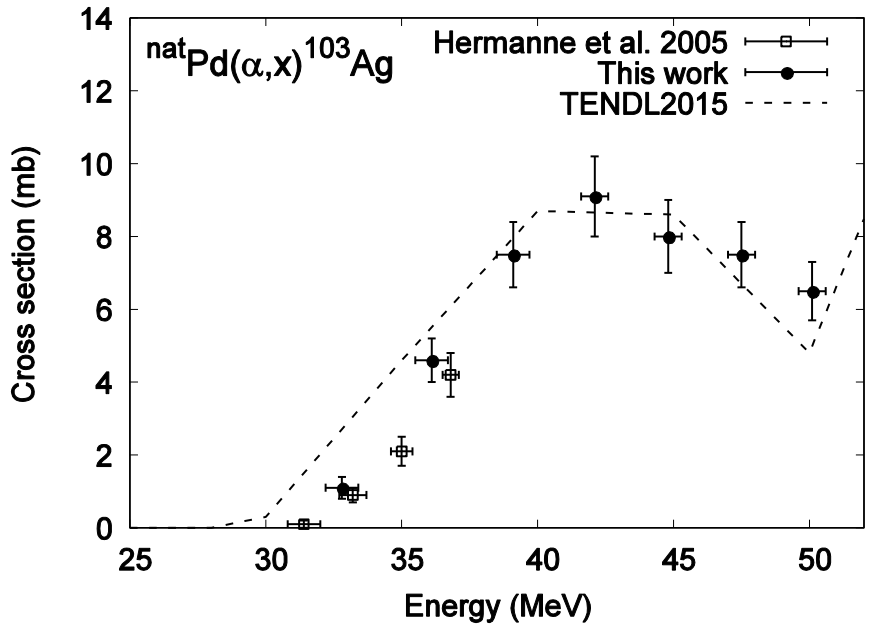

Fig. 1. The excitation function of the $^{nat}Pd(\alpha, x)^{103}Ag$ reaction. The result is compared with the previous experimental data [7] and TENDL-2015.

References

[1] S. Nag, D. Beyer, J. Friedland, P. Grimm, R. Nath, Int. J. Radiat. Oncol. Biol. Phys. 44 (1999) 789.

[2] A. Hermanne, S. Takács, F. Tárkányi, R. Bolbos, Radiochim. Acta 92 (2004) 215.

[3] Z. Szucs, J. van Rooyen, J. Zeevaart, Appl. Rad. Isot. 67 (2009) 1401.

[4] W. Meinke, Phys. Rev. 90 (1953) 410.

[5] C. Duncan and K. Krane, Phys. Rev. C 71 (2005) 054322.

[6] National Nuclear Data Center: the NuDat 2 database, http://www.nndc.bnl.gov/nudat2/.

[7] A. Hermanne, F. Tárkányi, S. Takács, Yu.N. Shubin, Nucl. Instr. Meth. B 229 (2005) 321.

[8] T. Watanabe, M. Fujimaki, N. Fukunishi, H. Imao, O. Kamigaito, M. Kase, M.

Komiyama, N. Sakamoto, K. Suda, M. Wakasugi, K. Yamada, Proc. 5th Int. Part. Accel. Conf. (IPAC2014), (2014) 3566.

[9] H.H. Andersen, J.F. Ziegler, Hydrogen Stopping Powers and Ranges in All Elements, Vol. 3, Pergamon, Oxford, 1997.

[10] F. Tárkányi, S. Takács, K. Gul, A. Hermanne, M.G. Mustafa, M. Nortier, P. Oblozinsky, S.M. Qaim, B. Scholten, Yu.N. Shubin, Z. Youxiang, IAEA TECDOC-1211, IAEA, Vienna, 2001, http://www-nds.iaea.org/medical.

[11] A.J. Koning, D. Rochman, J. Kopecky, J.C. Sublet, E. Bauge, S. Hilaire, P. Romain, B. Morillon, H. Duarte, S. van der Marck, S. Pomp, H. Sjostrand, R. Forrest, H. Henriksson, O. Cabellos, G. S., J. Leppanen, H. Leeb, A. Plompen, R. Mills, TENDL-2015: TALYS-based evaluated nuclear data library, https://tendl.web.psi.ch/tendl_2015/tendl2015.html.

Nuclear data measurement activities at CIAE

Xichao Ruan, Liyang Jiang, Yi Yang, Shilong Liu, Yangbo Nie, Zhaohui Wang, Xiongjun Chen, Weixiang Yu and Zhigang Ge

Key Laboratory of Nuclear Data, China Institute of Atomic Energy, Beijing 102413, China

Abstract. China Institute of Atomic Energy (CIAE) is one of the most important bases for nuclear data measurement in China. In this paper, the nuclear data measurement activities at CIAE in recent years are presented. The secondary neutron emission DX and DDX measurement, the integral experiment for nuclear data benchmarking, the excitation function measurement, the neutron induced fission yields measurement and the gamma production yields measurement carried out in recent years are introduced. Furthermore, the progress of some new facilities and proposed plans (e.g. A Gamma ray Total Absorption Facility (GTAF) for (n,γ) reaction cross section measurement, A ^{3}He detector array for (n,2n) reaction cross section measurement, the back streaming white neutron beam for nuclear data measurement at China Spallation Neutron Source (CSNS)) are also presented.

1 Introduction

The goal of nuclear data activities in China is supplying the nuclear data to feed the needs of the nuclear energy development, nuclear science study and nuclear technology applications. China Institute of Atomic Energy (CIAE) is one of the most important bases for nuclear data measurement in China. The facilities used for nuclear data measurement and study include the HI-13 tandem accelerator, 600kV-Cockcroft-Walton accelerator and 5SDH-2 2×1.7MV tandem accelerator. In addition, the China Experimental Fast Reactor (CEFR, 65 MW) reached critical on 21 June 2010, and China Advanced Research Reactor (CARR, 60MW, the maximum neutron flux: 8×10^{14}n/cm^{2}·s) reached critical on 13, May 2010 at CIAE, were also used for nuclear data related research. The China Spallation Neutron Source (CSNS)[1,2] will also be put into operation in 2018. A white neutron source beam line [3,4] based on CSNS will be available mainly for nuclear data measurement at that time. In this paper, the nuclear data measurement activities at CIAE in recent years are presented, and also the progress of some new facilities and proposed plans are given.

2 Recent Progress of Nuclear Data Measurement at CIAE

2.1 Excitation function measurements

1. ^{69}Ga(n,2n)^{68}Ga cross section measurements.

This measurement was performed with the 600 kV-Cockcroft-Walton accelerator in CIAE at the neutron energy of 14.1 and 14.9MeV with activation method. Based on the measurement, the existing experimental data of ^{69}Ga(n,2n)^{68}Ga cross section were reevaluated and a new evaluation was proposed based on CENDL-3.1. In this work, the most important finding is that the 511 keV gammas from the positron annihilation of ^{68}Ga are very difficultly measured accurately. Therefore the experimental data obtained by measuring 511 keV gammas are very difficult to measure accurately. And the branching ratio of ^{68}Ga decay should be re-evaluated [5].

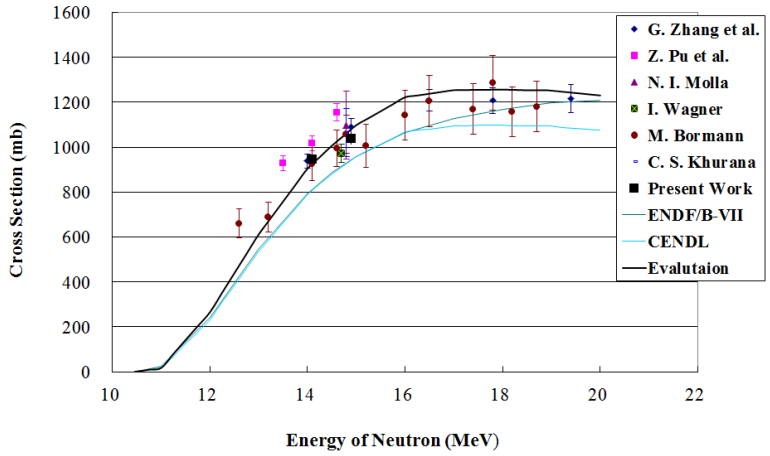

Fig. 1. Measured result of ^{69}Ga(n,2n)^{68}Ga cross section compared with other measurements and evaluations.

2. ^{241}Am(n,γ) cross section measurement at thermal energy.

The experiment was carried out to measure the cross section of ^{241}Am(n,γ)^{242g}Am reaction at the thermal neutron beam of 49-2 reactor in CIAE. The ^{241}Am sample was irradiated with a neutron beam with the flux of about 5×10^{10} n/cm^2/s. After irradiation, the alpha particles from ^{242}Am were measured with a silicon detector. The preliminary result proved that this cross section is measurable with current experimental conditions.

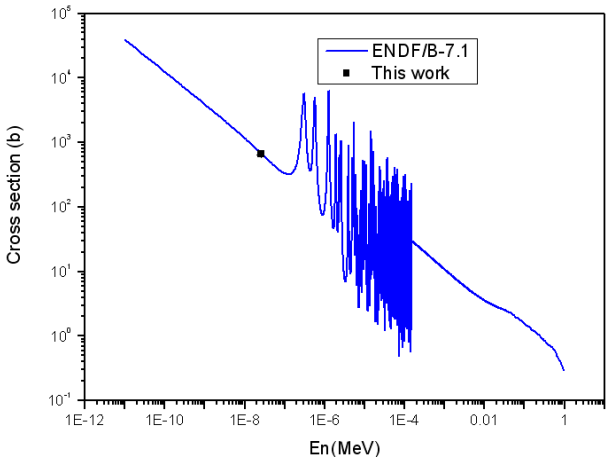

Fig. 2. The preliminary result of ^{241}Am(n,γ)^{242g}Am cross section at thermal energy.

2.2 Fission yield measurement

The fission yields of ^{235}U at 3 MeV, 14 MeV and ^{252}Cf spontaneous fission neutrons, ^{232}Th at 14 MeV neutrons were measured. Fission product activities were measured by a HPGe γ-ray spectrometer. Fission yields were determined by method of R-values relative to ^{140}Ba. Combined with previous measurements, part of the energy dependent fission yield for n+^{235}U fission reaction was shown in fig.3. One can see that the fission yields for some energy points can deviate from a linear function more than 10%. They agree with the systematic calculation result.

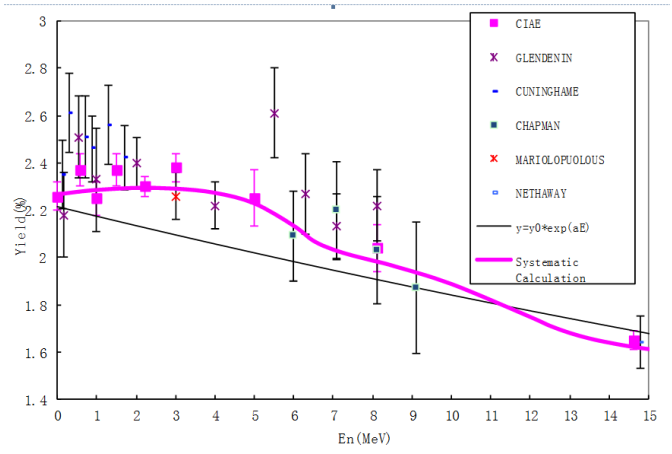

Fig. 3. Energy dependent fission yields of ^{147}Nd from ^{235}U fissions.

In addition, the technique for fission product mass yield distribution measurement is under development at CIAE. The E-v method of measuring the kinetic energy(E) and velocity(V) of outgoing fission products has been utilized, with the goal of

measuring the mass resolution better than 1 atomic mass units (amu), could identify every mass for light fission products of unsymmetrical fission.

2.3 The secondary neutron emission double-differential cross section measurement

The measurement of the double-differential cross sections (DDXs) of ^{9}Be at 22 and 25 MeV neutron energies and the measurement of DDXs of D at 8 MeV have been finished. These measurements are performed with the multi-detector fast neutron TOF spectrometer at the HI-13 Tandem Accelerator in CIAE. The diagram of the spectrometer is shown in Fig.4. The 22 MeV neutrons were produced by the T (d, n) ^{4}He reaction with a tritium gas target, while the 8 MeV neutrons were produced by D(d, n)^{3}He reaction with a deuterium gas target. The scattering samples were placed at 0° with respect to the deuteron beam about 20 cm away from the center of the gas target. A polyethylene sample was used to obtain the n-p scattering yield, and this yield was used for cross section normalization. More details about the experiments and the dada analysis can be found in Refs. [6-8].

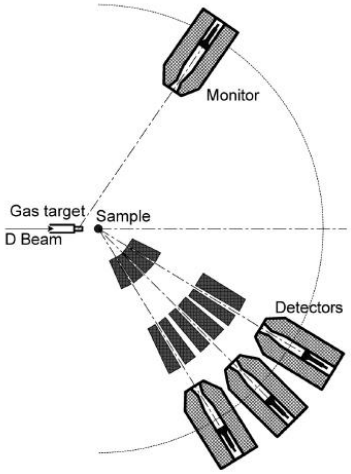

Fig. 4. Schematic view of the multi-detector fast neutron TOF spectrometer at CIAE.

Fig.5 shows part of the measured DDXs result of Be at 22 MeV, comparing with theoretical calculation with the LUNF code.

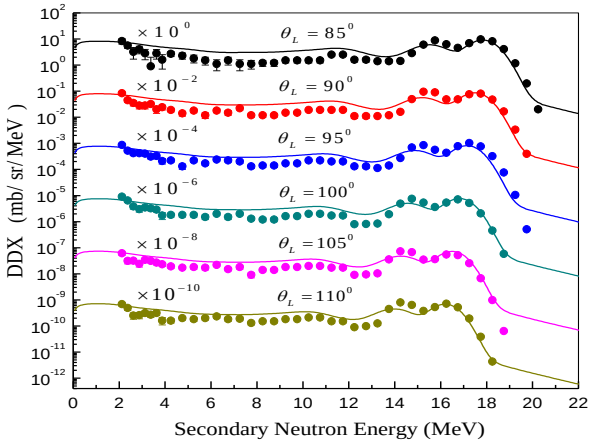

Fig. 5. Part of the measured DDXs for Be at 22 MeV.

2.4 The gamma production yields measurement

A HPGe detector array consists of 4 Clover detectors and 4 planar HPGe detectors was developed for this purpose. The detection system was used to measure the prompt γ rays from (n,xnγ) and (n,n'γ) reaction. Based on the 600kV-Cockcroft-Walton accelerator in CIAE, the measurements for ^{nat}Fe(n,n'γ) and ^{235,238}U(n,2nγ) have been carried out. Pulsed and direct current beam have been used to study the time dependent backgrounds. With the measurement of ^{nat}Fe target, the detection system was validated. In the experiment of ^{238}U target, A few γ rays from ^{238}U(n,xn) reactions have been observed, and the cross sections obtained are consistent with others' measurements. The data analysis of ^{235}U(n,xnγ) is ongoing.

Fig. 6. The HPGe detector array at CIAE.

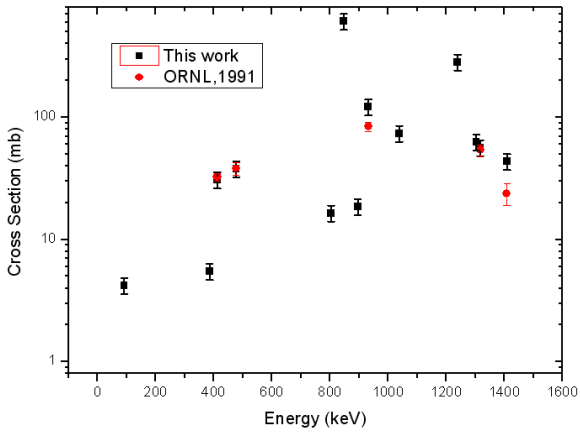

Fig. 7. The measured results for ^{56}Fe(n,n'γ).

2.5 Nuclear data benchmark experiments

The aim of the experiments is to make nuclear data benchmark for various important materials for the R&D of new generation nuclear energy systems such as CIADS (Chinese Initiative Accelerator Driven System) and TMSR in China. For this purpose, the neutron leakage spectra in the energy range from 0.8 to 15MeV from slab samples were measured by time-of-flight technique with a BC-501A scintillation detector. The measurements were performed at China Institute of Atomic Energy (CIAE) using a d-T neutron source. Fig.8 shows the experimental arrangement. The thicknesses of the slabs were 0.5 to 2.5 mean free path for 14.8 MeV neutrons, and the measured angles were chosen to be 60° and 120°. The measured spectra were compared with those calculated by the continuous energy Monte-Carlo transport code MCNP, using the data in the CENDL-3.1, ENDF/B-VII.1 and JENDL-4.0 nuclear data files. Table 1 list the measured samples in recent years. More details can be found in Refs.[9-12].

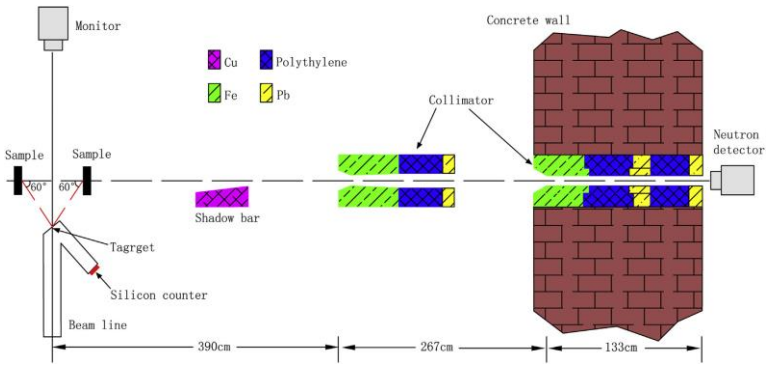

Fig.8. The experimental arrangement for the integral experiments.

Table 1. The measured samples.

Sample	Sample size/cm	Sample thickness/cm	Angle/°
^{238}U	10×10	5	45,135
Be	10×10	5, 11	60, 120
^{n}Ga	Φ13	3.2, 6.4	60, 120
^{n}W	10×10	3.5, 7	60, 120
Granular W	10×10	5	60
C	Φ13	20	60. 120
SiC	Φ13	20	60, 120
Pb	Φ13	5	60
Pb-Bi	Φ13	5	60
ThO_2	Φ13	5.4, 10.8	60, 120
H_2O	Φ13	5.2	60
PE	Φ13 10×10	6 5	60 45

3 New facilities for nuclear data measurement

3.1. The Gamma ray Total Absorption Facility (GTAF)

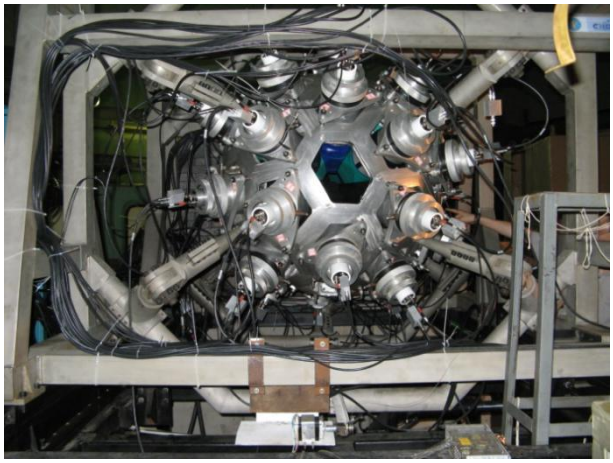

Fig.9. The GTAF facility at CIAE.

To feed the needs of neutron capture cross section measurement. The Gamma ray Total Absorption Facility (GTAF) has been constructed [13]. The detector consists of 40 BaF_2 crystals. The neutron capture event detection efficiency is expected to be more than 95% with this facility. The construction of this facility is now finalized and the test physics run is undergoing.

3.2 ^{3}He detector array for (n,2n) reaction cross section measurement

Traditionally, the activation method was used to measure the (n,2n) cross sections. The advantage of this method is that the experimental setup is simple and high precise data can be obtained. But the disadvantage is that the half-life of the compound nuclei has to be suitable for off-line measurement, which blocks the measurement of a lot of interesting nucleus. To overcome this disadvantage, a detector array consists of 100 ^{3}He proportional counters has been developed. Fig.10 shows the detector system. Spherical design was adopted to make the detection efficiency more independent of neutron energy. The neutron detection efficiency is about 30% for neutron energy below 5 MeV.

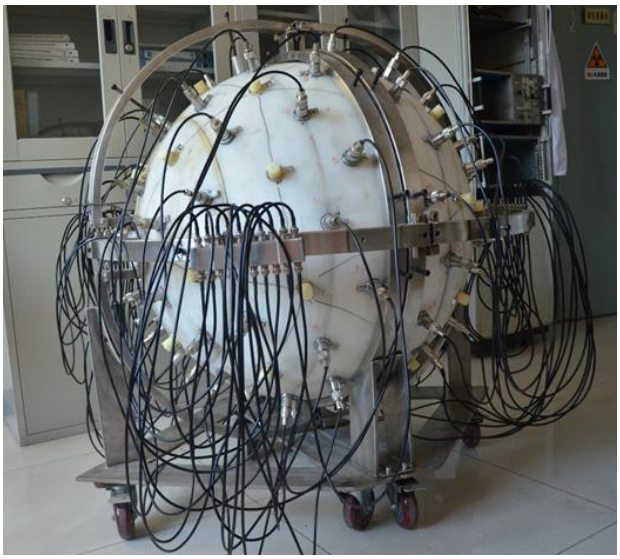

Fig.10. The ^{3}He detector array.

3.3 The back-streaming neutron beam line at CSNS

The China Spallation Neutron Source (CSNS) is a large scientific facility dedicated mainly to multidisciplinary research on material characterization using neutron scattering techniques. This project was officially approved by the Chinese central government in 2008, and will be in operation in 2018 for the 1st stage. In the first phase (CSNS-I), the machine will deliver 1.6 GeV protons on a tungsten target (TS1) with 100 kW beam power and a pulse repetition rate of 25 Hz. A back-streaming neutron beam line based on this machine was proposed and constructed mainly for nuclear data measurements.

A detailed study of the characteristics for the back-streaming neutrons at CSNS is described in ref.[4]. Based on this study, a nuclear data measurement program using the CSNS back-streaming neutron beam was proposed. The layout of the neutron beam tunnel and the experimental halls are shown in fig.11. Two end stations were constructed, with ~50 meters flight path for end station 1 and ~80 meters for end station 2, respectively. The end station 1 will be used for higher neutron flux required experiment while the end station 2 for better time resolution required experiment.In the first stage, the neutron total cross section measurement, capture cross section measurement with C6D6 detectors and fission cross section measurement with a normal ionization chamber are planed with this back-streaming neutron beam.

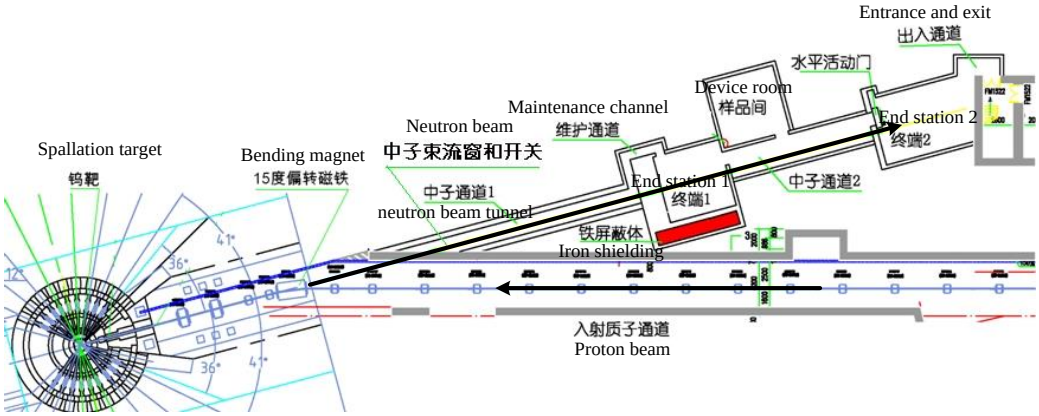

Fig.11. Layout of the CSNS back-streaming neutron beam tunnel and the experimental halls.

4 Conclusion

Substantial progress on nuclear data measurement has been made in China in recent years. More and more needs for nuclear data measurement have been required with the progress of the CIADS, TMSR and ITER projects in China. Some new facilities such as CSNS are under construction, these facilities will greatly improve the capability of the nuclear data measurement in China in the near future.

Acknowledgment

This work is supported by the Key Research Program from the Ministry of Science and Technology of China (2016YFA0401601) and the Advanced Research Project for nuclear data under grant No.4160303.

References

[1] S.X. Fang, et al., J. Kor. Phys. Soc. **48**, 697 (2006)

[2] Hesheng Chen, Xunli Wang, Nature Materials, **15**, 689 (2016)

[3] TANG Jing-Yu, FU Shi-Nian, JING Han-Tao, et al., Chinese Physics C, **34**(1), 121 (2010).

[4] H.T. Jing, J.Y. Tang,et al., Nuclear Instruments and Methods in Physics Research **A621**, 91 (2010).

[5] HUANG Xiao-long, JIANG Li-yang, CHEN Xiong-jun,et al. Chinese Physics C, **38**(4), 044001-1 (2014).

[6] Sa Jun, Tang Hongqing, Zhou Zuying, et al., Atomic Energy Sci. Technol. **26** (6) ,1 (1992) (in Chinese).

[7] Dankwart Schmidt, ZHOU Zu-Ying, RUAN Xi-Chao,et al. Nuclear Instruments and Methods in Physics Research, **A545**, 658(2005).

[8] RUAN Xi-chao, ZHOU Zu-ying, CHEN Guo-chang, et al. Chinese Physics C, **31**(5), 442 (2007).

[9] Y. Nie, J. Bao, et al. Ann. Nucl. Energy **37** (2010) 1456.

[10] R. Han, R. Wada, et al. Nucl. Phys. **A 936** (2015) 17.

[11] S. Zhang, Z. Chen, et al. Fus. Eng. Des. **92** (2015) 41.

[12] Y. Nie, J. Ren, et al. Fus. Eng. Des. **105** (2016) 8.

[13] ZHONG Qi-ping, ZHOU Zu-ying, TANG Hong-qing, et al. Chinese Physics C, **32** (suppl. II), 102 (2008).

Nuclear data activities using cyclotron and electron linac

Guinyun Kim[1], Kwangsoo Kim[1], Muhammad Zaman[1], Muhammad Sahid[1], Muhammad Nadeem[1], Manwoo Lee[2], Yeong-Rok Kang[2], Kyung Sook Kim[3], Sung Gyun Shin[3], Young Uk Kye[3], Moo-Hyun Cho[3], Sungchul Yang[4], Tae-Yung Song[4], Young-Ouk Lee[4], Hyungil Kim[4], and Tae-Ik Ro[5]

[1]*Department of Physics, Kyungpook National University, Daegu 702-701, Korea*
[2]*Research Center, Dongnam Institute of Radiological and Medical Sciences, Busan 619-953, Korea*
[3]*Division of Advanced Nuclear Engineering, Pohang University of Science and Technology, Pohang 790-784, Korea*
[4]*Nuclear Data Center, Korea Atomic Energy Research Institute, Daejeon 305-353, Korea*
[5]*Department of Physics, Dong-A University, Busan 604-714, Korea*

Measurement of charged particle-, neutron-, and photon-induced reactions are presented. Charged particle-induced reaction cross-sections are determined by using the stacked-foil activation technique at the MC-50 cyclotron facility in the Korean Institute of Radiological and Medical Science. Photon-induced nuclear data were measured by using the bremsstrahlung from the 100-MeV electron linac of Pohang Accelerator Laboratory. High-energy neutrons were produced from the ^{9}Be(p,n) reaction with 25-, 35-, and 45-MeV proton beam from the MC-50 Cyclotron at Korea Institute of Radiological and Medical Sciences (KIRAMS). The neutron-induced reaction cross-sections as a function of neutron energy were calculated using the TALYS 1.6.

We collaborated with foreign researchers in India, Japan, Russia, China, and Vietnam. We also utilized foreign facilities in India, Japan, Russia, and USA.

Recent nuclear data activities at KAERI

Young-Sik Cho*, Hyeong Il Kim, Sung-Chul Yang, Young-Ouk Lee

Nuclear Data Center, Korea Atomic Energy Research Institute, Korea

Nuclear Data Center at Korea Atomic Energy Research Institute (KAERI) is carrying out the nuclear data evaluation, processing, validation and measurement. The recent nuclear data activities including the cross section evaluations and the measurements at various facilities are briefly reported. The cross sections for the structural materials such as V, Cr and Ti, which are important in activation analysis of fusion reactor materials, have been evaluated. Measurements have been performed at the time-of-flight facility at GELINA to determine the $^{238}U(n,\gamma)$ cross section in the resonance region below 1.2 keV and between 3.5 keV and 90 keV. The production cross sections of radionuclides in the $^{89}Y(p,x)$ reactions were also measured at Korea Multi-purpose Accelerator Complex (KOMAC). The EXFOR compilation is one of KAERI's missions and the 8 domestic experimental data were recently compiled for the EXFOR database under the guidance of IAEA/NEA.

An evaluation of alpha-clustering in (n, α) reaction and alpha-decay

G. Khuukhenkhuu[1], M. Odsuren[1,2], S. Davaa[1], J. Munkhsaikhan[1] and E. Sansarbayar[1,3]

[1]*Nuclear Research Center, National University of Mongolia, Ulaanbaatar, Mongolia*
[2]*School of Engineering and Applied Sciences, National University of Mongolia, Ulaanbaatar, Mongolia*
[3]*Frank Laboratory of Neutron Physics, JINR, Dubna, Russia*

1. Introduction

Clustering in nuclei is an one of important subjects for understanding of light nuclear structure [1] α-particle [2] and heavy cluster decays [3] of nucleus ground states and cluster transfer and emission reactions [4]. Many authors have been considering for long time the clustering effect in nuclei using different approaches to this problem. Results of such studies are varied in the wide range depending on theoretical models used in the consideration.

In this work we suggest an unified view-point of the alpha-clustering problem for fast and slow neutron induced (n,α) reactions and ground-state α-decay of nuclei, namely, the statistical model[5] is utilized. The α-clustering factors obtained in this work are compared with other ones estimated from different assumptions.

2. Alpha-clustering in fast neutron induced (n,α) reactions

2.1. Statistical Model formula for Fast Neutron Induced Charged Particle Emission Reaction Cross Sections

In the framework of the statistical model based upon Bohr's postulate of the compound mechanism we use Weisskopf-Ewing evaporation model, constant nuclear temperature approximation [5] and concept of the nuclear entropy [6]. Then, can be gotten [7] following expression for fast neutron induced *x*-particle emission reaction cross section:

$$\sigma(n,x)=\sigma_c(n)\frac{2S_x+1}{2S_x+1}\frac{M_x}{M_n}e^{\frac{Q_{nx}-V_x}{\Theta}}. \quad (1)$$

Here:

$$\sigma_c(n)=\pi\left(R+\frac{\lambda}{2\pi}\right)^2 \quad (2)$$

is the compound nucleus formation cross section, where $R=r_oA^{1/3}$ is the target nucleus radius; A is the mass number of the target nucleus; λ is the wavelength of the incident neutrons; S_x, S_n, M_x and M_n are the spin and mass of the outgoing *x*-particle and neutron, respectively; Q_{nx} is the (*n*,*x*) reaction energy; V_x is the Coulomb potential of the *x*-particle; $\Theta=kT$ is the nuclear thermodynamical temperature, where *k* is the Boltzmann constant and *T* is the absolute temperature.

The Weizsäcker's formula for binding energy [8] of the target and residual nuclei can be used to obtain the reaction energy Q_{nx} in formula (1). The Coulomb potentials of proton and α-particle can be determined by Gardner's formulas [9,10]. The thermodynamical temperature Θ is obtained using the Fermi gas model [11]:

$$\Theta=\sqrt{\frac{13.5(E_n+Q_{nx})}{A^*}}, \quad (3)$$

where E_n is the neutron energy; A^* is the residual nucleus mass number.

Thus, the following formula for fast neutron induced (n,p) reaction cross section can be obtained from (1):

$$\sigma(n,p)=C\pi\left(R+\frac{\lambda}{2\pi}\right)^2\exp\left(-K\frac{N-Z+1}{A}\right) \quad (4)$$

Here:

$$C=\exp\frac{1}{\Theta}\left(\gamma\frac{2Z-1}{A^{1/3}}-V_p\right) \quad (5)$$

and

$$K = \frac{4\xi}{\Theta}, \tag{6}$$

where: N and Z are the neutron and proton numbers, respectively; γ and ξ are the Weizsacker's formula constants;

Also, fast neutron induced (n,α) reaction cross section is expressed by analogy to (n,p) cross section as following:

$$\sigma(n,\alpha) = C\pi\left(R + \frac{\lambda}{2\pi}\right)^2 \exp\left(-K\frac{N-Z+0.5}{A}\right). \tag{7}$$

Here:

$$C = 2\exp\frac{1}{\Theta}\left(-3\alpha + \beta\left(A^{2/3} - (A-3)^{2/3}\right) + \gamma\left(\frac{Z^2}{A^{1/3}} - \frac{(Z-2)^2}{(A-3)^{1/3}}\right) + \varepsilon_\alpha - V_\alpha\right) \tag{8}$$

and

$$K = \frac{2\xi}{\Theta}, \tag{9}$$

where: α and β are the Weizsäcker's constants; ε_α=28.2 MeV is the internal binding energy of α-particle.

2.2. The Comparison of Theoretical and Experimental Cross Sections

2.2.1. (n,p) Cross Sections

Theoretical values calculated by statistical model formula (4), (6) and experimental data for (n,p) cross sections at neutron energies of 8 and 16 MeV are compared in Fig.1, as examples.

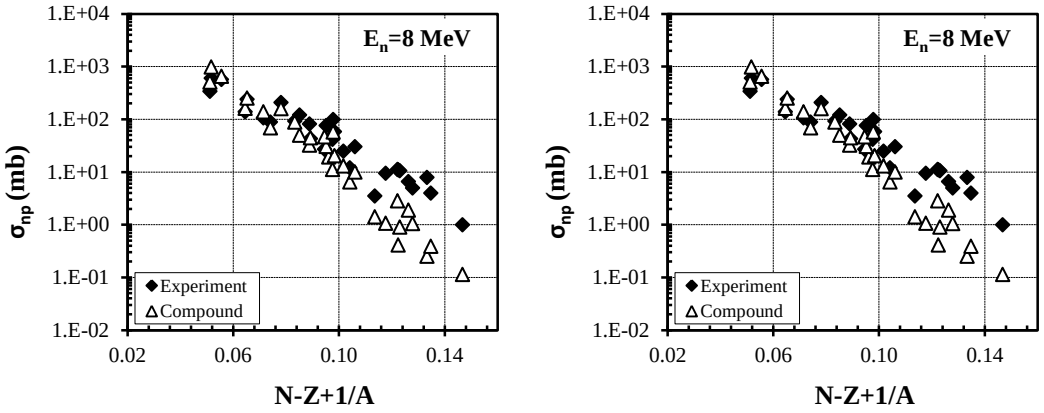

Fig. 1. Theoretical and experimental (n,p) cross sections for neutron energy of 8 and 16 MeV.

It is seen that calculated by statistical model cross sections and experimental data are satisfactorily in agreement with some deviation. Similar results were obtained for wide neutron energy range of 2 to 20 MeV [7,12,13]. This fact means that the statistical model roughly describes fast neutron induced (n,p) reaction cross sections.

2.2.2. (n,α) Cross Sections

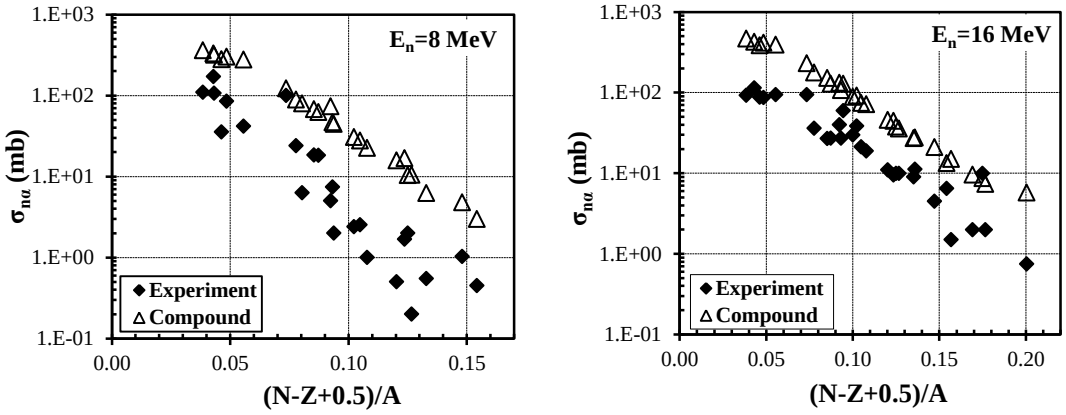

Fig. 2. The same as in Fig.1 for (n,α) reactions.

2.2.3 The (n,α) cross sections and alpha-clustering factor

Theoretical (n,α) cross sections calculated by formula (7), (9) and experimental

data for neutron energy of 8 and 16 MeV are given in Fig.2, as examples. Fig.2 shows that statistical model formula (7) and (9) give overestimated values for the (n, α) cross sections at energy points of 8 and 18 MeV. Similar discrepancies between the theoretical and experimental (n, α) cross sections were observed for other neutron energy range of 2 to 20 MeV [14,15]. These results, possibly, are caused by the α-particle clustering effect.

As mentioned above, statistical model formula (4) and (6) are correct and give satisfactory results for fast neutron induced (n,p) reaction cross sections. At the same time theoretical (n,α) cross sections calculated by statistical model formula (7) and (9) are in disagreement with experimental data. From here we concluded that the difference between the theoretical and experimental (n,α) cross sections is caused by α-clustering effect because in the derivation of the theoretical formula (7) and (9) the surface α-clustering from four nucleons of the mother nucleus is not taken into account. However many attempts were carried out [1-4, 16-27], determination of the α-clustering probability up to now is not completely solved.

Here we suggest some simple relative method to find α-clustering factor for fast neutron induced (n, α) reactions, namely, this factor is obtained by normalizing of theoretical (n, α) cross sections to experimental data. This method means that α-clustering factor is determined in comparison with nucleon (proton) emission probability. If the α-clustering effect will be taken into account the (n, α) cross section formula (7) can be rewritten in the form:

$$\sigma(n,\alpha) = C\pi\left(R + \frac{\lambda}{2\pi}\right)^2 \phi_\alpha \exp\left(-K\frac{N-Z+0.5}{A}\right), \qquad (10)$$

where ϕ_α is the α-clustering factor which is obtained as following:

$$\phi_\alpha = \frac{1}{W_{p/\alpha}} = \frac{\sigma^{\exp}_{(n,\alpha)}}{\sigma^{th}_{(n,\alpha)}} = \frac{\sigma^{\exp}_{(n,\alpha)}}{C\pi\left(R + \frac{\lambda}{2\pi}\right)^2 \exp\left(-K\frac{N-Z+0.5}{A}\right)}. \qquad (11)$$

Average values of the α-clustering factor at each neutron energy point are obtained as an inverse quantity of the normalizing coefficient (see formula (11) and Fig.3) for theoretical and experimental (n, α) cross sections at E_n = 8 and 16 MeV, as

examples.

$W_{p/\alpha}$ is the normalizing coefficient Values of the α-clustering factors obtained by using the same method for different neutron energy of 2 to 20 MeV are given in Table 1.

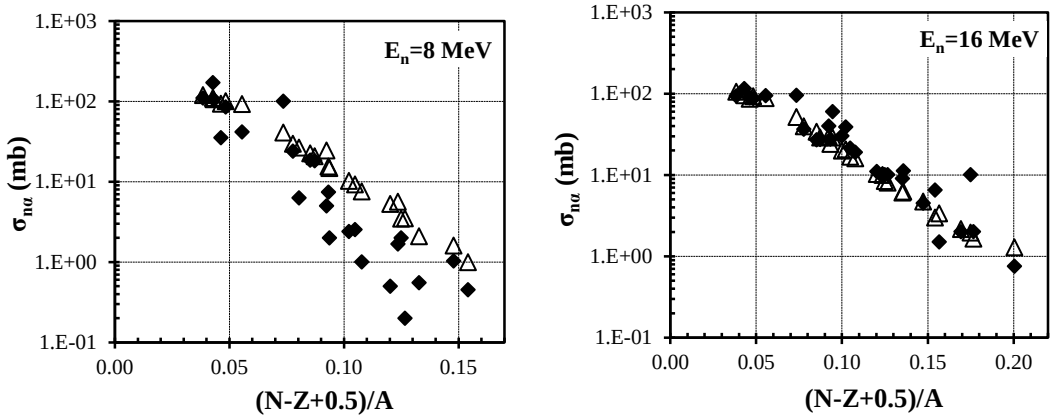

Fig. 3. Normalized theoretical and experimental (n, α) cross sections for 8 and 16 MeV.

Table 1. The values of α-clustering factor for different neutron energy.

E_n (MeV)	2	4	4.5	5	5.5	6	6.5	8	10	13	14.5	16	18	20
$W_{p/\alpha}$	50	4.5	4.5	4.0	3.5	3.5	3.5	3.0	3.0	3.0	3.5	4.5	5.5	10
ϕ_α	0.02	0.22	0.22	0.25	0.28	0.28	0.28	0.33	0.33	0.33	0.28	0.22	0.18	0.1

The dependence of the α-clustering factor ϕ_α on neutron energy E_n is shown in Fig.4. It is seen that the α-clustering factor ϕ_α is increased up to E_n=10 MeV after that is decreased. Also, It can be seen that our values $\phi_\alpha = 0.1 \div 0.33$ except E_n=2 MeV ($\phi_\alpha = 0.02$) are close to results of Popov et al. for slow neutrons[17-19] and to α-particle preformation probability of Bonetti and Milazzo-Colli [20].

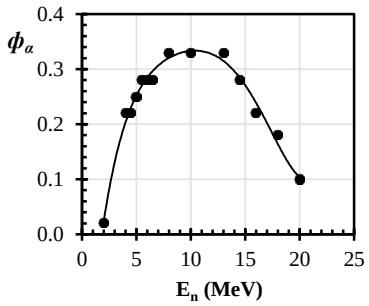

Fig. 4. The energy dependence of the α-clustering factor for fast neutron induced (n,α) reactions.

3. Alpha-clustering in slow neutron induced (n,α) reactions

3.1. Theoretical formula

In the framework of the statistical model and taking into account the α-clustering factor the total α-width can be written in the following form:

$$\Gamma_\alpha = \hbar f_\alpha T_\alpha \phi_\alpha , \tag{12}$$

where f_α is the frequency of the α-particle motion in the daughter nucleus potential barrier; T_α is the transmission factor. The frequency f_α can be firstly obtained by following formula [5]:

$$f_\alpha = \frac{D}{2\pi\hbar}, \tag{13}$$

where D is the average level distance. Secondly, the frequency f_α is determined using the α-particle classical kinetic energy inside potential well:

$$f_\alpha = \frac{1}{\tau_\alpha} = \frac{1}{\left(\frac{2R}{\upsilon_\alpha}\right)} = \frac{1}{R}\sqrt{\frac{E_\alpha}{2m_\alpha}}, \tag{14}$$

where τ_α is the period of the motion; υ_α is the α-particle velocity; E_α is the α-particle energy; m_α is the α-particle mass and R is the daughter nucleus radius.

The α-clustering factor can be obtained from (12) and (14) by two methods:

$$\phi_\alpha = 2\pi \frac{\Gamma_\alpha}{DT_\alpha} \tag{15}$$

and

$$\phi_\alpha = \frac{\Gamma_\alpha}{\hbar T_\alpha c} r_0 (A_D^{1/3}) \sqrt{\frac{2m_\alpha (MeV)}{E_\alpha (MeV)}} \tag{16}$$

where c is the light velocity; A_D is the daughter nucleus mass number.

3.2 Alpha-Clustering Factor for Slow Neutron Induced (n,α) Reactions

The formulas (15) and (16) are used to calculate α-clustering factor ϕ_α for slow neutron induced (n,α) reactions. Values of the total alpha-width Γ_α were taken from (n,α) reaction data for resonance neutrons by Popov *et al.*[19] as average experimental α-widths $\langle \Gamma_\alpha^{\exp} \rangle$ because the total α-width has some fluctuation.

The transmission factor T_α was calculated by Rasmussen formula [28,29]. The average level spacings D in formula (15) were chosen by different ways:

1. As nuclear surface vibration quantum energy[30]: $D_s \approx 1$ MeV;

2. Average distance between the α-cluster levels in the daughter nucleus potential[23]: $D_\alpha \approx 20$ MeV;

3. From Fermi gas model and preformed α-particle model of nuclear reactions[20]:

$$D_F = \frac{4}{g_0} = \frac{4}{\left(\frac{6}{\pi^2} a\right)} = \frac{2\pi^2 13.5}{3A} MeV, \tag{17}$$

where: g_0 is the single particle level density of the Fermi gas model[11].

Results of our calculations for the α-clustering factor of the slow neutron induced (n,α) reactions for some isotopes are given in Table.2. It is seen from Table.2 that the α-clustering factors varied from ~10^{-3} to ~10^{-7}, which are satisfactorily in agreement with Kadmensky and Furman cluster model conclusions: 7×10^{-4}, 3×10^{-5} and 8×10^{-7}

for favoured, semifavoured and unfavoured α-transitions, respectively. At the same time, our calculations show that cluster model level spacing D_α=20 MeV [3] gives lower values of ϕ_α than other two cases (Fermi gas $D_F=4/g_0$ and D_s=1 MeV).

Table 2. Alpha-clustering factors from slow neutron induced (n,α) reactions.

Compound nuclei		N*	$\langle\Gamma_\alpha^{exp}\rangle$ (μeV) [19]	E_α (MeV)	l_α	T_α	ϕ_α, by formula (15)			ϕ_α, by formula (16)
Isotope	J^π						D_s= 1 MeV	D_α= 20 MeV	$D_F=\frac{4}{g_0}$	
^{65}Zn	1/2	1	12	3.626	1	6.24E-08	1.2E-03	6.0E-05	8.7E-04	2.2E-04
^{68}Zn	3^-	6	580	4.578	3	5.54E-06	6.6E-04	3.3E-05	5.0E-04	1.1E-04
^{96}Mo	2^+	4	26	6.127	2	7.87E-07	2.1E-04	1.0E-05	2.2E-04	3.4E-05
^{124}Te	0^+	7	7.3	7.331	0	2.32E-07	2.0E-04	9.9E-06	2.7E-04	3.2E-05
^{144}Nd	3^-	15	21	9.453	3	1.49E-06	8.9E-05	4.4E-06	1.4E-04	1.3E-05
^{146}Nd	3^-	5	0.32	8.507	3	4.84E-08	4.2E-05	2.1E-06	6.8E-05	6.7E-06
^{148}Sm	3^-	20	2.3	9.856	3	1.75E-06	8.3E-06	4.1E-07	1.4E-05	1.2E-06
^{150}Sm	3^-	13	0.21	9.183	3	1.85E-07	7.1E-06	3.6E-07	1.2E-05	1.1E-06

*N: Number of resonances

4. Alpha-clustering in the alpha-decay

4.1. formula

Alpha-decay rate can be written as following

$$\lambda_\alpha = \phi_\alpha f_\alpha T_\alpha = \frac{0.693}{T_{1/2}}. \tag{18}$$

From (18) the α-clustering factor is determined by

$$\phi_\alpha = \frac{0.693}{f_\alpha T_\alpha T_{1/2}}. \tag{19}$$

Here we can use formula (13) and (14) for the frequency f_α. Then the α-clustering

factor will be expressed as follows:

$$\phi_\alpha = \frac{0.693h}{DT_\alpha T_{1/2}} \tag{20}$$

and

$$\phi_\alpha = \frac{0.693 r_0 A_D^{1/3}}{T_\alpha T_{1/2} c} \sqrt{\frac{2m_\alpha(MeV)}{E_\alpha(MeV)}}\,. \tag{21}$$

4.2. Alpha-clustering in the Alpha-decay

The values of the α-clustering factors calculated by formula (20) and (21) for α-decay of some rare earth and heavy elements are given in Table.3.

Table 3. Alpha-clustering factors for α-decay.

Isotope	E_α (MeV)	$T_{1/2}$ (s)	T_α	ϕ_α, by formula (20)			ϕ_α, by formula (21)
				D_s= 1MeV	Cluster model D_α= 20 MeV	$D_F = \frac{4}{g_0}$	
^{144}Nd	1.83	7.1E22	4.98E-45	8.07	0.4	13.07	2.77
^{146}Sm	2.45	3.2E15	5.69E-37	1.57	0.07	2.58	0.47
^{147}Sm	2.23	3.3E18	4.97E-40	1.75	0.08	2.88	0.55
^{148}Sm	1.96	2.2E23	1.74E-44	0.75	0.03	1.24	0.25
^{210}Po	5.307	1.2E07	8.27E-27	0.03	0.001	0.07	0.0066
^{226}Ra	4.78	5.0E10	6.43E-32	0.89	0.04	2.26	0.22
^{234}U	4.77	7.7E12	3.82E-34	0.97	0.05	2.56	0.25
^{238}U	4.2	1.4E17	1.48E-38	1.38	0.07	3.69	0.37
^{238}Pu	5.5	2.7E09	1.9E-30	0.56	0.03	1.49	0.13
^{239}Pu	5.16	7.6E11	1.6E-32	0.24	0.01	0.63	0.057
^{240}Pu	5.17	2.1E11	1.94E-32	0.71	0.03	1.92	0.17
^{242}Pu	4.9	1.2E13	3.23E-34	0.74	0.04	2.01	0.19

Table.3 shows that values of the α-clustering factors calculated by formula (17) and (20), and with D_s=1 MeV are $\phi_\alpha \geq 1$ which are not real. At the same time, the formula (20) with D_α=20 MeV and formula (21) give ϕ_α<1 except α-decay of ^{144}Nd.

These results are close to our values of the ϕ_α for fast neutron induced (n,α) reactions. It can be seen, also, that our calculated α-clustering factors for the slow neutron induced (n,α) reactions and α-decay are essentially different.

5. Conclusions

1. In the framework of the statistical model we found the α-particle formation factor for fast neutron induced (n, α) reactions normalizing the theoretical cross sections to experimental data. This method means that α-clustering factor is determined in comparison with proton (nucleon) emission probability.

2. The α-particle formation factors were obtained for α-decay and slow neutron induced (n, α) reactions using the statistical model, also. The values of α-clustering factor for slow neutron induced (n,α) reactions are close to theoretical results of Kadmensky and Furman.

3. It was shown that our values of α-clustering factor for fast neutron induced (n, α) reactions and the α-decay are close to the Popov et al.[17-19] and Bonetti and Milazzo Colli [20] results.

References

[1] K.Wildermuth and Y.C.Tang, A Unified Theory of the Nucleus. Vieweg Braunschweig, 1977.

[2] S.G.Kadmensky and V.I.Furman, Alpha-decay and Related Nuclear Reactions, "Energoatomizdat", Moscow, 1986, (in Russian)

[3] Yu.S.Zamyatnin, V.L.Mikheev, S.P.Tretyakova et al., Physics of Elementary Particles and Atomic Nuclei, v.21, part.2, JINR, 1990, Dubna, p.537 (in Russian)

[4] P.E.Hodgson, Alpha-clustering in Nuclei, Chapter 23 of "The Uncertainty Principle and Foundations of Quantum Mechanics". Editors: W.C.Price and S.S.Chissick, New York, John Wiley, 1977, p.485

[5] J.M.Blatt and V.F.Weisskopf, Theoretical Nuclear Physics, New York, John Wiley

and Sons, 1952

[6] L.Landau, Ya.Smorodinsky, Lectures of Atomic Nuclear Theory, TTL, Moscow, 1955 (in Russian)

[7] G.Khuukhenkhuu, G.Unenbat, M.Odsuren *et al.*, Communication of the JINR, E3-2007-25, Dubna, 2007

[8] C.F.Weizsäcker, Z. Phys., v.96 A, N7-8, 1935, p.431

[9] D.G.Gardner and S.Rosenblum, Nucl.Phys., v.96A, N1, 1964, p.121

[10] D.G.Gardner and Yu-Wen Yu, Nucl.Phys., v.60, N1, 1964, p.49

[11] A.Bohr and B.R.Mottelson, Nuclear Structure, v.1, New York-Amsterdam,

W. A. Benjamin, Inc., 1969

[12] G.Khuukhenkhuu, M.Odsuren, Yu.M.Gledenov and M.V.Sedysheva, Journal of the Korean Physical Society, v.59, N2, 2011, p.851

[13] G.Khuukhenkhuu, Yu.M.Gledenov, M.V.Sedysheva and M.Odsuren, Proceedings of the XVI International Seminar on Interaction of Neutrons with Nuclei, JINR, 2009, Dubna, p.255

[14] G.Khuukhenkhuu, M.Odsuren, J.Munkhsaikhan *et al.*, Proceedings of the XXIV International Seminar on Interaction of Neutrons with Nuclei, JINR, 2016, Dubna, p.(in Press)

[15] G.Khuukhenkhuu, Yu.M.Gledenov, M.V.Sedysheva *et al.*, Physics of Elementary Particles and Atomic Nuclei, Letters, v.11, N6 (190), 2014, p.749

[16] H.A.Bethe, Nucl. Phys. B, Nuclear Dynamics, Theoretical, Rev. Mod. Phys., v.9, N2, 1937

[17] Yu.P.Popov, M.Pshitula, K.G.Rodionov *et al.*, Yad.Fiz., v.13, N5, 1971, p.913

[18] Yu.P.Popov and V.I.Furman, In book: III School of Neutron Physics, JINR, 1978, Dubna, p.390

[19] N.P.Balabanov, V.A.Vtyurin, Yu.M.Gledenov and Yu.P.Popov, Physics of

Elementary Particles and Atomic Nuclei, v.21, N2, 1990, p.317

[20] R.Bonetti and L.Milazzo-Colli, Phys.Lett., v.49B, N1, 1974, p.17

[21] T.Knellwolf and J.Rossel, Helv.Phys.Acta, v.39, N4, (1966), p.376

[22] J.I.Hogan, Z.Phys., v.295 A, N2, 1980, p.169

[23] S.G.Kadmensky and V.I.Furman, Physics of Elementary Particles and Atomic Nuclei, v.6, part.2, 1975, p.469, (in Russian)

[24] I.Tonozuka and A.Arima, Nucl.Phys., v.323 A, 1979, p.45

[25] A.Iwamoto and K.Harada, Phys.Rev., v.26C, N5, 1982, p.1821

[26] H.F.Zhang and G.Royer, Phys.Rev., v.77C, N5, 2008, p.054318

[27] H.F.Zhang, G.Royer and J.Q.Li, Phys.Rev., v.84 C, N2, 2011, p.027303

[28] J.O.Rasmussen, Phys. Rev., v.113, N6, 1959, p.1593

[29] T.Delgersaikhan, G.Khuukhenkhuu, M.Odsuren and J.Munkhsaikhan, Scientific Transactions, Physics, NUM, N362 (17), 2012, p.158

[30] B.N.Andreev and S.M.Sirotkin, Yad.Fiz., v.1, N2, 1965, p.252

Review of fission yields measurements in China Nuclear Data Center

J. Feng[1], Y. Yang[1], S. Liu[1], Y. Liu[1], Z. Lee[1], A. Cui[1]

[1]*China Nuclear Data Center, Beijing 102413, China*

The fission yields measurements in CNDC can be divided as 2 periods. before and after 1990s. For the first period, Radio-chemistry and RC-gamma ray spectrometry (RC-GeLi) methods are applied to get fission yields. Since then, HpGe spectrometry become the method mainly adopted with the developing of semiconductor technology. In first period, we measured thermal, Fission, 3MeV, 5MeV, 8MeV, 14MeV, 14.7MeV and 14.9MeV neutron induced fission of ^{235}U and ^{238}U. It is important to state that the fission rates are monitored by a double fission chamber which has 2 standard Uranium samples to count the rates before and after the neutron penetration. Figure 1 shows one of the results for ^{238}U from fission neutron.

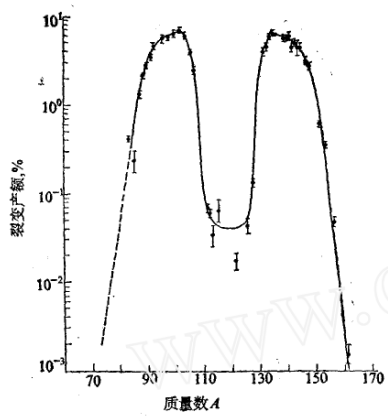

Fig. 1. Product Yields of ^{238}U from fission neutron

After 1990s, the group extended inducing neutron energy to 0.57MeV, 1.0MeV, 1.5Mev, 11.3MeV, 19MeV and 22MeV. 14.8MeV for ^{232}Th and Thermal for ^{239}Pu experiments were also carried out in this period. Figure 2 shows the mass distribution change of different neutron energy induced fission of ^{235}U.

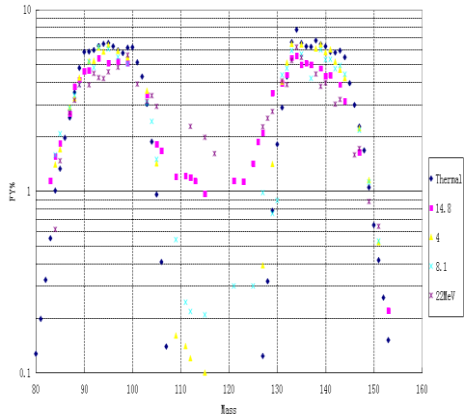

Fig. 2. Mass distribution of ^{235}U fission from different neutron energies.

The group also has interest in depicting the behavior of fission yields with some mathematical and physical ideas. Figure 3 shows a 5 Gaussian approaching of the mass distribution for ^{235}U, the neutron emission is taking into account to reflect different Q value from different neutron energies. Figure 4 shows the result of the fitting for several product yields.

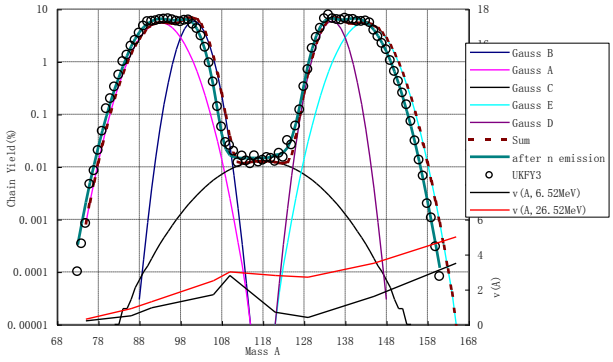

Fig. 3. Five Gaussian fitting for mass distribution of ^{235}U fission.

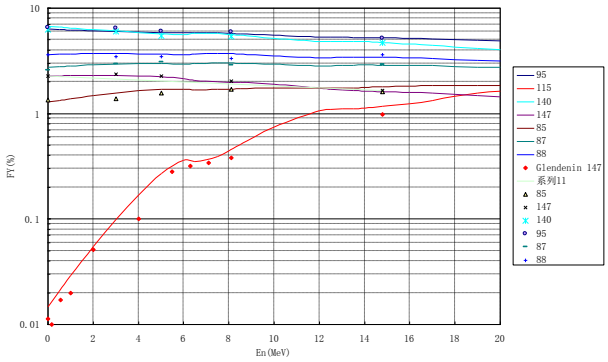

Fig. 4. Five-Gaussian fitting result for several product mass of ^{235}U.

We acknowledge Prof. H. Lu, Prof. Z. Zhou and Prof. W. Yu for their enthusiasm in improving the experimental precision.

References

1. Feng Jing,et al., 99Mo yields from 0—2MeV neutron induced fission of 235U, Atomic Energy Science and Technology, Vol 48(9),2013

2. Yang Yang, Feng Jing et al., Determination of Nuclear fission number by delayed high-energy γ rays. Atomic Energy Science and Technology, Vol 47(4),2013

3. Feng Jing, Yang Yi et al., 95Zr，140Ba and 147Nd Yields from 0.57,1.0 and 1.5MeV neutron induced fission of 235U.Journal of nuclear and radiochemistry, Vol32(6),2010

4. Bao Jie, et.al.,Fission counts measurements by delayed neutron method, Atomic energy Sci & Tec,1479,s9(2013).

5. Yang Yi, et.al. ,~(235)U/~(238)U abundance ratio measurement by fission yields ratio. Atomic energy Sci & Tec,1-3,s1(2012)

6. Guo shuqing; Feng Jing; Han Hongying; Liu Shilong, Estimation of U/239(n,f) Cross Section by U/238(O/18,O/16f),Annual report of china institute of atomic energy,124-125(2011)

Evaluation of ^{186}W(d,2n)^{186}Re reaction cross sections

Jimin Wang, Xi Tao, Mengxiao Kang, Xiaolong Huang, Youxiang Zhuang

China Nuclear Data Center, China Institute of Atomic Energy, 102413 Beijing, China

Rhenium-186 is an important medically radionuclide, and regarded very suitable for radiotherapy and radio immunotherapy due to its attractive properties which include emission of high-energy β-rays 1.07MeV, low-abundance (9.42%) γ emission at 137 keV, and 90.64 h half-life.

The ^{186}Re has been produced using nuclear reactors through ^{185}Re(n,γ)^{186}Re reaction, but the specific activity is medium, not in no-carrier-added form. In order to radiolabel antibodies more efficiently, production of no-carrier-added ^{186}Re with high specific activity is required. There are two major routes for the production of no-carrier-added ^{186}Re by cyclotron, namely ^{186}W(p,n)^{186}Re and ^{186}W(d,2n)^{186}Re.

In the present work, the excitation function of ^{186}W(d,2n)^{186}Re reaction was evaluated and recommended below 50 MeV on basis of least-squares fit with orthogonal polynomial and the theoretical calculation. The available experimental data from EXFOR library and literature were analyzed and corrected with the γ-rays branch ratio, radioactive decay constant and standard cross sections. The available experimental data include the latest reports [1, 2] that are not considered in previous works [3, 4]. The nuclear model calculation was done using TALYS [5]. The thick target yield (TTY) of therapeutic radioisotope ^{186}Re was calculated using the recommended excitation function of ^{186}W(d,2n)^{186}Re reaction, and compared with the TTY from ^{186}W(p,n)^{186}Re reaction [6].

Eight experiments [1-2, 7-12] of ^{186}W(d,2n)^{186}Re reaction were founded in EXFOR library and literature, listed in **Table 1** and shown in **Fig. 1**. The experimental data were normalized to 100% enrichment of ^{186}W, considering the given enrichment of the target in the literature and the isotopic composition of natural tungsten, i.e. ^{180}W (0.12%), ^{182}W (26.50%), ^{183}W (14.31%), ^{184}W (30.64%) and ^{186}W (28.43%). In the measurements of F. Tarkanyi et al. [11], K. Ochiai et al. [12], S. Manenti et al. [1] and C. Duchemin et al. [2], the samples were thick natural W-metal foils, so the

normalization factor is 3.517. In the measurement of F.W. Pement et al. [8], the sample was WO_3 powder, enriched to 97.2% in ^{186}W, so the normalization factor is 1.0288.

Table 1. Measurements of $^{186}W(d,2n)^{186}Re$ reaction.

Years	Author	Institute	Sample	Method	Subentry
1966	F.W. Pement et al.[8]	USAPUP	WO_3 enriched to 97.2%	STTA	P0115 007
1973	S.J. Nassiff et al. [9]	GERKFK	—	STTA, ACTIV	A0202 004
1981	Tao Zhenlan et al.[7]	CPRNRS	WO_3 enriched to 99%	STTA, ACTIV	S0014 003
2002	N.S. Ishioka et al. [10]	JPNJAE	natural	STTA, ACTIV	E2083 002
2003	F. Tarkanyi et al.[11]	HUNDEB BLGVUB	natural	STTA, ACTIV	D4141 007
2007	K. Ochiai et al.[12]	JPNJAE JPNJPN	natural	STTA, ACTIV	E2121 025
2014	S. Manenti et al.[1]	ITYMIL ZZZISP	natural	STTA, ACTIV	O2224 008
2015	C. Duchemin et al.[2]	FRNTE	natural	STTA, BCINT	O2258 002

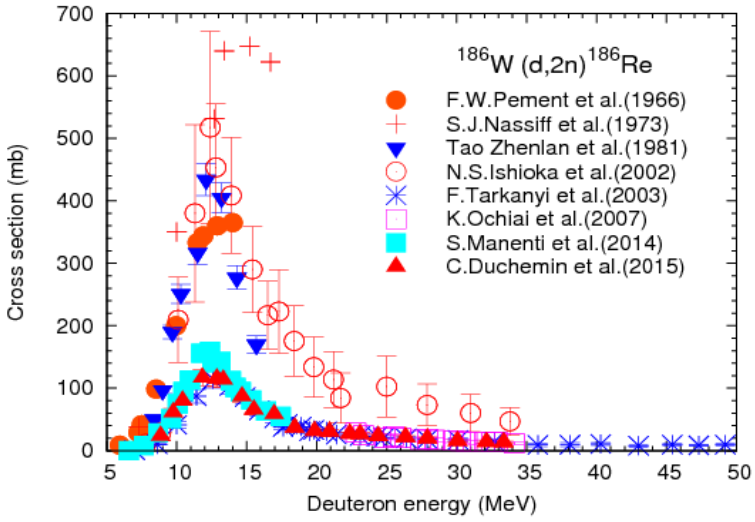

Fig. 1. Original experimental data.

In the measurement of Tao Zhenlan et al. [7], the γ-rays branching ratio of 137.16 keV are 0.092, and the new value is 0.0942 [13]. The sample was WO_3 powder, enriched to 99% in ^{186}W, so the corrected factor is 0.9813. The experimental data after normalization and correction are shown in **Fig. 2**.

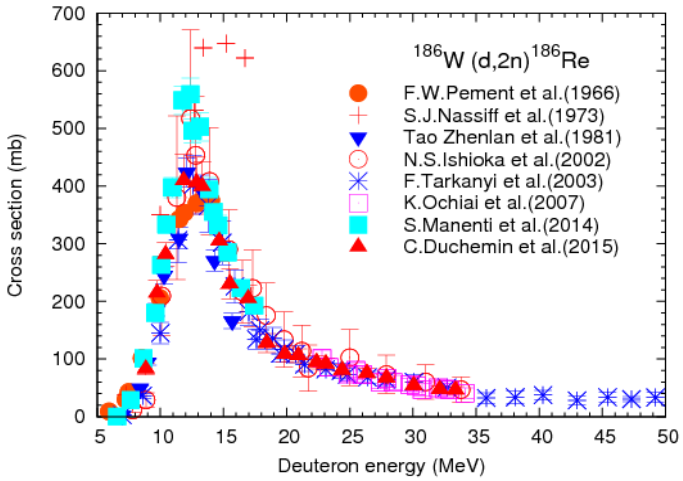

Fig. 2. The experimental data after normalization and correction.

Several nuclear model code have been developed, in the evaluation of data are very helpful. In the process of evaluation, the parameters of the nuclear model code need to be adjusted to reproduce the experimental data. In this work, the cross sections were calculated using TALYS, a nuclear model code, developed by Koning et al. [5]. The nuclei were considered non-spherical in shape. The compound nucleus contribution was considered in the frame of Moldaner model. The contributions of direct reactions were taken into account by ECIS. The back-shifted Fermi gas model (BFM) was used for level densities (ldmodel 2). The OM parameters were adjusted, the parameter RVADJUST was set to 1.2. The pairing energy of ^{186}Re was set to 0.0. The theoretical results are shown in **Fig. 3**.

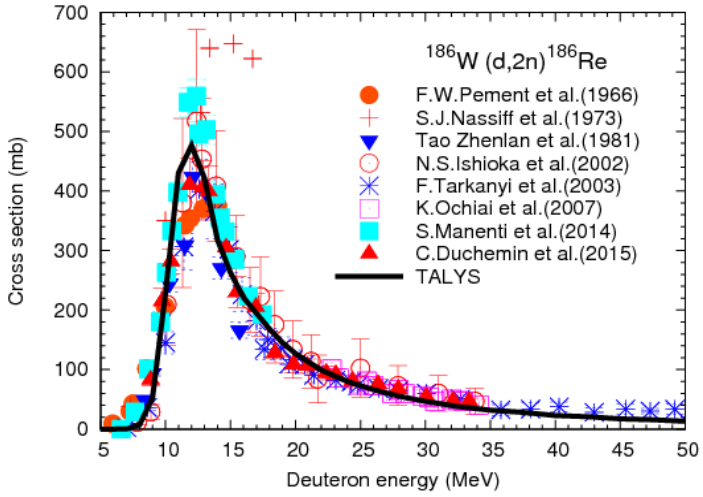

Fig. 3. The results of nuclear model calculation using TALYS.

After normalization and correction, the experimental data are consistent besides the partial data of S.J. Nassiff et al. [9] and S. Manenti et al. [1]. S.J. Nassiff et al. reported six cross section values from 7.3 to 16.7 MeV, but the errors not given. The data are higher than the calculated values using TALYS and those reported by other authors between 10 to 20 MeV. The data of S. Manenti et al. are higher than the results of calculation and other measurements at 11.76, 12.38, 12.54 and 13.14 MeV. F.W. Pement et al. [8] reported nine data points but not given the errors also. So these data were neglected in fitting of experimental data.

On basis of least-squares fit with orthogonal polynomial, the evaluated experimental data were fitted from threshold to 14 MeV and from 14 to 50 MeV. The curves of fitting are shown in **Fig. 4** and **Fig. 5**.

The function of fitting from threshold to 14 MeV as follows:

$$\sigma_{d,2n} = a - bE_d + cE_d^{\,2} - dE_d^{\,3} \tag{1}$$

Where, a = 4.2176, b = 1.4378, c = 0.1555, d = 0.0052.

The function of fitting from 14 to 50 MeV as follows:

$$\sigma_{d,2n} = \exp(a - bE_d + cE_d^{\,2}) \tag{2}$$

Where, a = 1.8248, b = 0.2544, c = 0.0031.

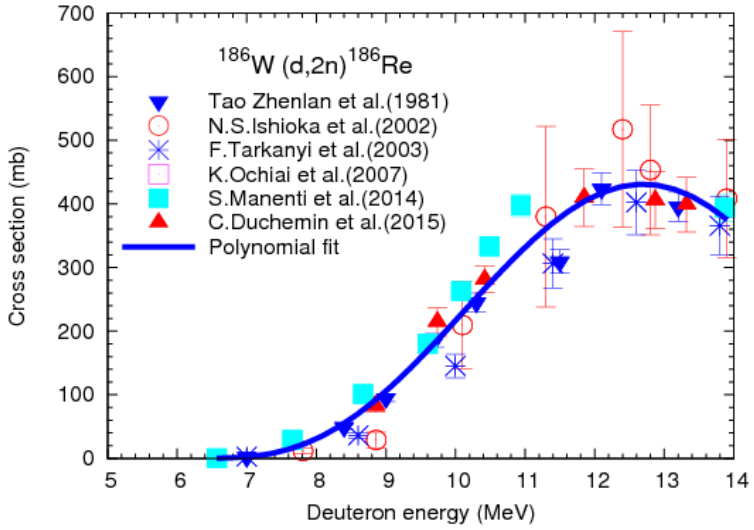

Fig. 4. The results of fitting from threshold to 14 MeV.

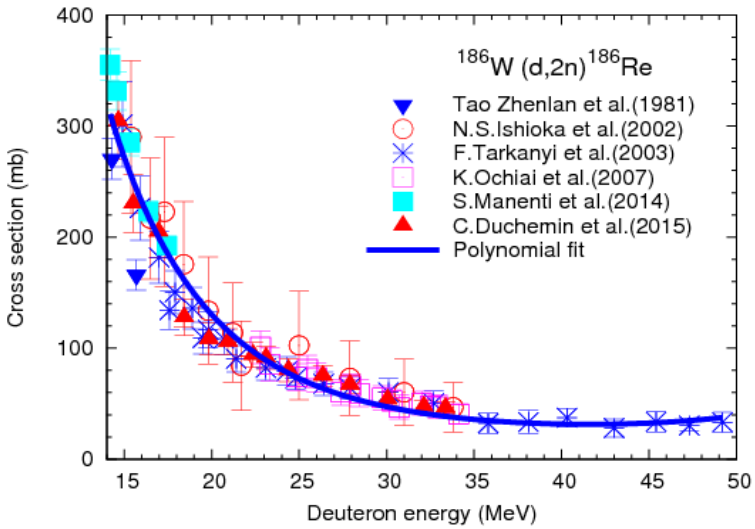

Fig. 5. The results of fitting from 14 to 50 MeV.

The excitation function for ^{186}W(d,2n)^{186}Re reaction was recommended from threshold energy to 50 MeV after comprehensive evaluation , take into account the results of calculation and fitting. The recommended curve is given in **Fig. 6**, together with the results of M. Hussain et al. [3] and IAEA TRS 473 [4]. The recommended excitation function of ^{186}W(d,2n)^{186}Re reaction are agree with the experimental data, the maximum value is 4.8% higher than the value of IAEA TRS 473, and 4.7% lower than the value of M. Hussain et al.

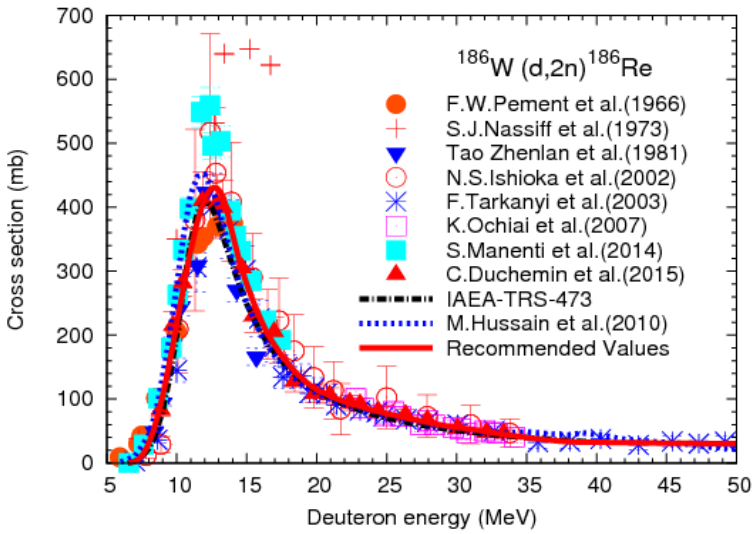

Fig. 6. The recommended excitation function for ^{186}W(d,2n)^{186}Re reaction, compared with experimental data and results published earlier.

The thick target yield (TTY) of ^{186}Re was calculated using the recommended excitation function of ^{186}W(d,2n)^{186}Re reaction, and compared with the TTY from ^{186}W(p,n)^{186}Re reaction [6], together with the measurements [1, 14-15] are shown in **Fig. 7.** The TTY of ^{186}W(d,2n)^{186}Re reaction are much higher than the value of ^{186}W(p,n)^{186}Re reaction above 15 MeV. So the ^{186}W(d,2n)^{186}Re reaction may be more suitable for production of no-carrier-added ^{186}Re for medical application, if the deuteron beams are available by cyclotron and the energy is high enough.

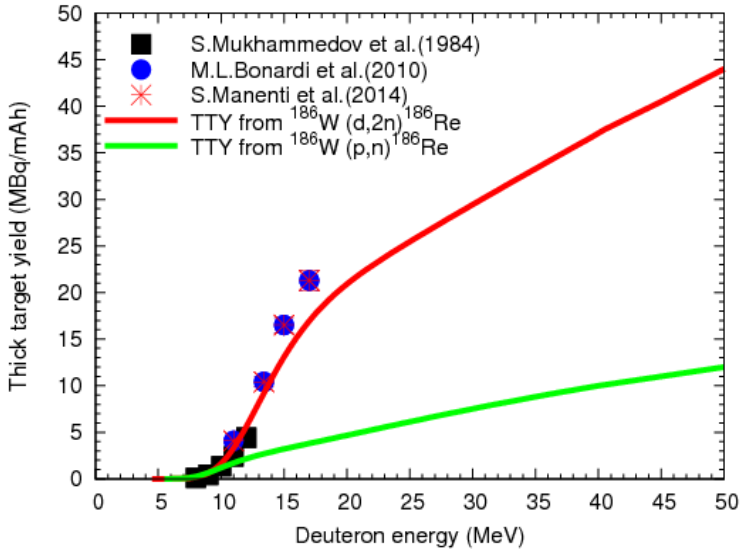

Fig. 7. The TTY of ^{186}W(d,2n)^{186}Re reaction, compared with the TTY of ^{186}W(p,n)^{186}Re reaction.

References

[13] S. Manenti, E. Persico, K. Abbas, M.L. Bonardi, L. Gini, F. Groppi, U. Holzwarth, F. Simonelli, Radiochimica Acta, 102 (2014) 669, EXFOR O2224.

[14] C. Duchemin, A. Guertin, F. Haddad, N. Michel, V. Metivier, Applied Radiation and Isotopes, 97 (2015)52, EXFOR O2258.

[15] M. Hussain, S. Sudar, M.N. Aslam, R. Ahmad, A.A. Malik, S.M. Qaim, Radiochimica Acta, 98 (2010) 385, EXFOR D0730.

[16] S.M. Qaim, F. Tarkanyi, R. Capote, IAEA-TRS-473, 328 (2011).

[17] A.J. Koning, S. Hilaire and M.C. Duijvestijn, EDP Sciences, 211, (2008).

[18] Mengxiao Kang, Xiaolong Huang, Lile Liu, Atomic Energy Science and Technology, 50(2016)2114, (in Chinese).

[19] Zhenlan Tao, Fuying Zhu, Huiyuan Qiu, Gongqing Wang, Chinese Journal of Nuclear Physics, 3 (1981) 242, EXFOR S0014.

[20] F.W. Pement, R.L. Wolke, Nuclear Physics, 86 (1966) 429, EXFOR P0115.

[21] S.J. Nassiff, H. Munzel, Radiochimica Acta, 19 (1973) 97, EXFOR A0202.

[22] N.S. Ishioka, S. Watanabe, A. Osa, M. Koizumi, H. Matsuoka, T. Sekine, Journal of Nuclear Science and Technology, Supplement 2 (2002) 1334, EXFOR E2083.

[23] F. Tarkanyi, S. Takacs, F. Szelecsenyi, F. Ditroi, A. Hermanne, M. Sonck, Nuclear Instruments and Methods in Physics Research B, 211 (2003) 319, EXFOR D4141.

[24] K. Ochiai, M. Nakao, N. Kubota, S. Sato, M. Yamauchi, N.H. Ishioka, T. Nishitani, C. Konno, EDP Sciences, 1011, (2008), EXFOR E2121.

[25] Xiaolong Huang, Zhigang Ge, Zhendong Wu, Guochang Chen, Jimin Wang, Xi Tao, Jianhui Li, V.P. Chechev, S.A. Badikov, T.V. Golashvilli, O.O. Patarakin, V.I. Rachkov, Nuclear Characteristics of Nuclides, China Atomic Energy Press, 2013.

[26] S. Mukhammedov, A. Vasidov, E. Pardaev, Soviet Atomic Energy, 56 (1984)56, EXFOR A0212.

[27] M.L. Bonardi, F. Groppi, S. Manenti, E. Persico, L. Gini, Applied Radiation and Isotopes, 68 (2010) 1595, EXFOR D0623.

Low energy scattering cross sections for n + ^{6}Li and n + ^{7}Li reactions

D. Ichinkhorloo [1], M. Aikawa [2], S. Chiba [3], Y.Hirabayashi [4], and K. Katō [2]

[1]*Meme Media Laboratory, Hokkaido University, Sapporo 060-8628, Japan*

[2]*Nuclear Reaction Data Centre, Faculty of Science, Hokkaido University, Sapporo 060-0810, Japan*

[3]*Research Laboratory for Nuclear Reactors, Tokyo Institute of Technology, Tokyo 152-8550, Japan*

[4]*Information Initiative Center, Hokkaido University, Sapporo 060-0811, Japan*

Abstract. We study the integrated elastic and inelastic scattering cross sections together with their angular distributions n+ ^{6,7}Li using n + (α + d) and n + (α +t) cluster models, respectively, and the continuum-discretized coupled-channel framework. The microscopic single-folding potential is used for the neutron energies from 1 to 24 MeV. The calculated elastic and inelastic scattering cross sections are in good agreement with experimental and evaluated data for the observed incident energies.

1. Introduction

The n + Li reactions have attracted a lot of attention not only from the basic interest but also from the application point of view. Lithium isotopes will be used as a tritium-breeding material in $d - t$ fusion reactors. Therefore accurate nuclear data are required for n-induced reactions of ^{6,7}Li.

In the previous works [1–3], we have successfully studied cross sections for the n + ^{6,7}Li elastic and inelastic scattering angular distributions and neutron spectra applying the continuum-discretized coupled-channel (CDCC) method [4] assuming n + (α + d) and n + (α + t) models. It was found that the calculated cross sections for incident energies from 7.47 to 24 MeV can be reproduced by their cluster models with one normalization factor for the imaginary part of the n − ^{6,7}Li folding potential of the

complex Jeukenne-Lejeune-Mahaux effective nucleon-nucleon (JLM) [5] interaction. More recently, Guo *et al.* [6] have analyzed both neutron and proton scatterings from ^{6,7}Li in a wide incident-energy range up to 150 MeV, and demonstrated the applicability of the CDCC to nucleon scattering from ^{6,7}Li. They analyzed neutron total cross sections, proton reaction cross sections, and differential cross sections of nucleon elastic and inelastic scatterings. However, it is still difficult to reproduce the data at energy lower than about 10 MeV in their frameworks.

In this work, we extend the CDCC analysis of the integrated elastic and inelastic scattering cross sections of n + Li with incident neutron energies below 14.1 MeV using the JLM which was proposed for an energy region lower than 10 MeV [7]. This is because of the fact that the different kinds of the parameter sets are defined for the JLM effective nucleon-nucleon interaction in lower and higher energy regions [5,7]. Furthermore, we employ the normalization factors to adjust folding potentials of the JLM for the n + ^{6,7}Li elastic scattering in a similar way as the previous studies [1–3]. The energy-dependent normalization factors λ_v and λ_w for real and imaginary parts, respectively, of the n − ^{6,7}Li folding potentials are determined from the integrated elastic cross section data.

Using the obtained normalization factors, we calculate the inelastic scattering cross sections and angular distributions and compare the results with the experimental data without any additional parameters. Recently, a new experiment of the inelastic neutron scattering cross section to the first excited state in ^{7}Li was measured by Nyman *et al.* [8]. We discuss the comparison between the experimental, evaluated data and our CDCC calculations.

2. The Method and Model

We prepare the wave functions of the bound and α-d,t scattering states of ^{6,7}Li in the similar way as previous work [1-3] in the CDCC method.

In ^{6}Li case, the binding energy of the 1^{+} ground state is observed as 1.47 MeV with respect to the ^{6}Li$\rightarrow$ α + d threshold, and the low-energy part of the α-d scattering phase shifts in the S-wave (ℓ=0) and D-wave (ℓ=2) have been obtained

experimentally. The excited 3^+, 2^+ and 1^+ states of ^{6}Li are observed at 2.18, 4.31, and 5.68 MeV, respectively, which are considered to be the triplet resonance state in the α-*d*, *D*-wave. According to the cluster model, the wave functions for the ground state (1^+) and the exited states are written as

$$\phi_{\ell I}(^6Li;k) = A\left\{\varphi(\alpha)[\varphi_I(d)\otimes u_\ell(k,\ r)]_I\right\}, \tag{1}$$

where $\varphi(\alpha)$ and $\varphi_I(d)$ stand for the internal wave functions of the alpha and deuteron clusters, respectively.

The interaction between α and *d* has central and spin-orbit parts, which are parametrized by a two-range Gaussian form and by a two-range Gaussian-derivative form, respectively;

$$V^{CE}{}_\ell(r) = \upsilon_{1,\ell}e^{-(r/r_{1,\ell})^2} + \upsilon_{2,\ell}e^{-(r/r_{2,\ell})^2} + V_{CL}(r)$$

$$V_\ell^{SO}(r) = \upsilon_{1,\ell}^{SO}re^{-(r/r_{1,\ell})^2} + \upsilon_{2,\ell}^{SO}re^{-(r/r_{2,\ell})^2} \tag{2}$$

$$V_{CL}(r) = \begin{cases} Z_1Z_2e^2/r, & r \geq R_{CL} \\ \left(Z_1Z_2e^2/(2R_{CL})\right)\left(3-r^2/R_{CL}{}^2\right), & r < R_{CL}. \end{cases}$$

They are chosen ℓ-dependently so as to reproduce well the energies of the ground and excited states and the α-*d* scattering phase shifts. The parameter values are listed in Table 1.

Table 1. The parameters of the effective central and spin orbit potentials between α and *d* for ℓ = 0 and 2.

Parameters	$r_{1,\ell}$ (fm)	$r_{2,\ell}$ (fm)	$\upsilon_{1,\ell}$ (MeV)	$\upsilon_{2,\ell}$ (MeV)	$\upsilon_{1,\ell}^{(SO)}$ (MeV)	$\upsilon_{2,\ell}^{(SO)}$ (MeV)	R_{CL} (fm)
ℓ = 0	2.191	1.607	-105.85	46.22	--	--	3.00
ℓ = 2	2.377	1.852	-82.00	26.00	-2.31	1.42	3.00

The Schrödinger equation of the n + ^{6}Li scattering system, which is described by using the n + α + *d* three body model, is written as

$$\left[K_R + K_r + V_{d\,\alpha}(r) + \sum_{i\in\alpha,d} \upsilon_{in} - E \right] \Psi_{JM}^{CDCC} = 0 \,, \tag{3}$$

where E is the energy of the total system, vector $\vec{r}$ is the relative coordinate between α and d, $\vec{R}$ the one between the center of mass of the d-α pair and n. Operators $K_{\rm r}$ and $K_{\rm R}$ are kinetic energies associated with $\vec{r}$ and $\vec{R}$, respectively, and $V_{d\alpha}(\vec{r}\,)$ is the interaction between d and α. $\sum_{i\in\alpha,d}\upsilon_{in}$ is the interaction between incident neutron and the ith nucleon in α and d clusters where is υ_{in} an effective nucleon-nucleon interaction. The total wave function Ψ_{JM} with the total angular momentum J and its projection M on z-axis is expanded in terms of the orthonormal set of eigenstates $\phi_{\ell I}$ of $H(^6{\rm Li})$ for the α-d system;

$$\Psi_{JM}^{CDCC}(\vec{r},\vec{R}) = \sum_{L} Y_{JM}^{\ell_0 I_0 L} \phi_0(r) \hat{\chi}_{\gamma_0}(P_0,R)/R$$

$$+ \sum_{i=1}^{N} \sum_{\ell=0}^{\ell_{\max}} \sum_{I} \sum_{L} Y_{JM}^{\ell I L} \hat{\phi}_{i\ell I}(r) \hat{\chi}_{\gamma}(\hat{P},R)/R, \tag{4}$$

where the spin and angular parts are described as

$$Y_{JM}^{\ell I L} = \left[[i^{\ell} Y_{\ell}(\Omega_r) \otimes \eta_d \,] \otimes i^{\ell} Y_L(\Omega_R) \right]_{JM} \varphi(\alpha)\varphi(d), \tag{5}$$

with

$$\hat{\chi}_{\gamma_0}(P_0,R) = \chi_{\gamma_0}(P_0/R), \quad \gamma_0 = (0,\ell_0,I_0,L,J) \tag{6}$$

$$\hat{\chi}_{\gamma}(\hat{P}_{\gamma},R) = W_{\gamma}\chi_{\gamma}(\hat{P}_{\gamma}/R), \quad \gamma = (i,\ell,I,L,J)$$

On the right hand side of Eq.(4), the first term presents the elastic channel denoted by γ_0 and the second one corresponds to the discretized breakup channels, each denoted by γ. The expansion-coefficient χ_{γ} in Eq.(6) represents the relative motion between n

and ^{6}Li, and L is the orbital angular momentum regarding $\vec{R}$. The diagonal and coupling potentials for n + ^{6}Li systems are calculated by folding the JLM effective nucleon-nucleon interaction in the same way as Ref. [3].

Table 2. The parameters of the effective central and spin orbit potentials between α and t for ℓ =1 and 3.

Parameters	$r_{1,\ell}$ (fm)	$r_{2,\ell}$ (fm)	$v_{1,\ell}$ (MeV)	$v_{2,\ell}$ (MeV)	$v_{1,\ell}^{(SO)}$ (MeV)	$v_{2,\ell}^{(SO)}$ (MeV)	$r_{1,\ell}^{(SO)}$ (fm)	$r_{2,\ell}^{(SO)}$ (fm)
ℓ =1 (3/2$^-$)	2.447	--	-84.70	--	-0.99	-0.67	4.900	2.447
ℓ =1 (1/2$^-$)	2.447	--	-89.50	--	-0.30	-0.11	4.900	2.447
ℓ = 3	2.608	--	-75.65	--	-1.05	--	2.466	2.447

In ^{7}Li case, we prepare the wave functions of the bound and α-t scattering states of ^{7}Li in the similar way as the ^{6}Li + n reaction analysis in the CDCC method. The binding energy of the 3/2$^-$ and 1/2$^-$ bound states are observed as -2.47 MeV and -1.99 MeV, respectively, with respect to the ^{7}Li$\rightarrow$ α + t threshold, and the low-energy part of the α-t scattering phase shifts in the P-wave (ℓ =1) and F-wave (ℓ = 3) have been obtained experimentally. The excited 7/2$^-$ and 5/2$^-$ states of ^{7}Li are observed at 4.65 MeV and 6.60 MeV, which are considered to be the triplet resonance state in the α-t relative motion with the F-wave.

The potential between α and t clusters is chosen ℓ-dependently so as to reproduce well the energies of the ground state, and the excited states, and the α-t scattering phase shifts. The parameters are listed in Table 2.

3. Results and discussion

We analyze the integrated elastic and inelastic cross sections of the n + ^{6}Li scattering. Here, we describe the inelastic resonant state of ^{6}Li using discrete basis functions in the CDCC framework. Because the resonant state has a distribution over

an energy range of the resonance width around the resonance energy E_r, we calculate the inelastic cross section of n +^{6}Li for a resonant state of ^{6}Li taking a sum of the breakup cross sections of n + (α + d) for several discretized solutions obtained in the resonance energy region. In the n + ^{6}Li scattering, we calculate the inelastic cross section for the 3^+ resonant state of ^{6}Li at the 2.18-MeV excitation energy by taking a sum of three solutions obtained around the resonance energy of the α + d system.

We first take the normalization factors λ_v= 1.0 and λ_w= 0.2 to reproduce the observed integrated elastic scattering cross sections data from 1 to 24 MeV as shown in Fig. 1, where the calculated results are presented by the dotted line (JLM-1). These values for λ_v and λ_w indicate that the small imaginary potential is needed while the real part has no adjustment parameter. This is almost consistent with λ_v= 1.0 and λ_w= 0.1 in the previous studies [1–3], and means that the CDCC framework of the n + (α + d) model well describes the n +^{6}Li scattering. But we cannot reproduce experimental data of the lower incident neutron energy region for elastic scattering cross sections as shown in Fig. 1.

Table 3. The normalization factors λ_v and λ_w for real and imaginary parts, respectively, of the n −^{6}Li folding potential.

E_n (MeV)	λ_v	λ_w	E_n (MeV)	λ_v	λ_w
1.0	1.256	0.0	7.0	1.060	0.1
2.0	1.277	0.0	8.0	1.060	0.1
3.0	1.242	0.0	9.0	1.040	0.15
4.0	1.235	0.0	10.0	1.030	0.2
5.0	1.160	0.0	11.0	1.020	0.2
6.0	1.120	0.0	≥11.5	1.000	0.2

Second, we try to readjust normalization factors λ_v and λ_w so as to reproduce the low energy data of the measured integrated elastic cross section below 11.5 MeV. The obtained normalization factors for each energy are presented in Table 3, and the

calculated integrated elastic cross sections are shown by the solid line (JLM-2) in Fig. 1. As seen from Table 3, λ_v for the real part of the potential becomes larger than 1.0 but the imaginary part λ_w goes to zero. The integrated elastic cross section is very sensitive to values of λ_w in lower energies. We indicate this sensitivity by the grey area in Fig. 3 where the upper and lower lines of the integrated elastic cross sections are calculated for $\lambda_v \pm 0.01$.

As shown in Fig. 1, it is noticed that the calculated integrated elastic cross sections show a good agreement with the evaluated data (JENDL-3.3) [14] for the n + ^{6}Li scattering. After fixing the parameters of λ_v and λ_w , we try to calculate the integrated inelastic scattering cross section and angular distributions of the elastic and inelastic scattering to see the reliability of these parameter values.

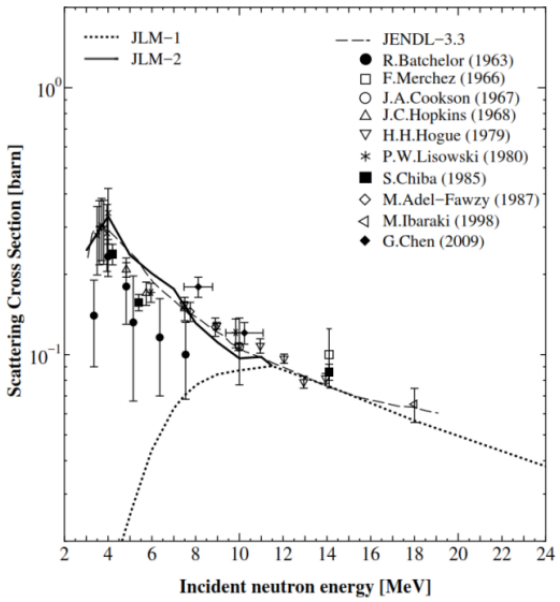

Fig. 1. The integrated elastic cross sections of the n + ^{6}Li scattering, in comparison with the evaluated data [14] and experimental data [15–23].

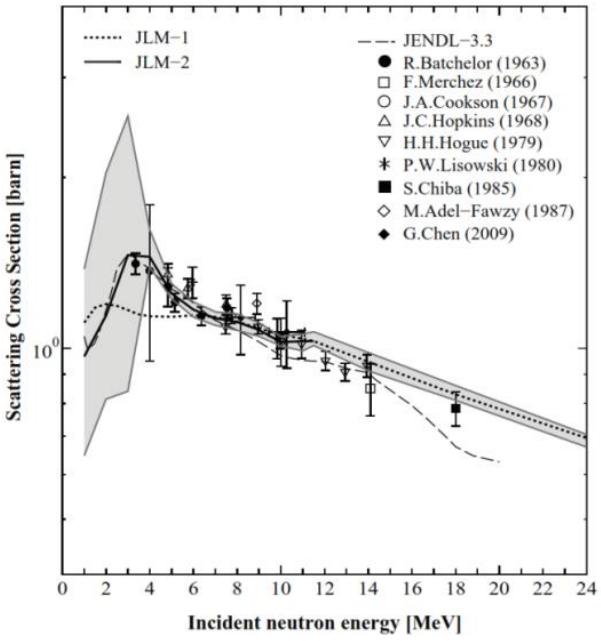

Fig. 2. The integrated inelastic n + 6Li scattering cross sections for the excited 3+ state at the excitation energy of 2.18 MeV of Li in comparison with the evaluated data [14] and experimental data [15–25].

We calculate the integrated inelastic cross sections for the 2.18 MeV state of ^{6}Li, and show the results together with the experimental data in Fig. 2. When we calculate them with an energy-independent normalization factors we obtain the result (JLM-1) of a fall-off behavior in lower energies, which show a large deviation from the observed data. On the other hand, the energy-dependent normalization factors bring about a very good result in comparison with the experimental data and the evaluation data of JENDL-3.3.

Using the same energy-dependent normalization factors, we calculate the angular distributions. Figure 3 shows the results of calculations and experiments of the differential cross sections of the n +^{6}Li elastic scattering with incident energies between 4.0 and 24.0 MeV. One can see that the results of the CDCC calculation represented with the solid line are in good agreement with the experimental data. For inelastic scattering, Fig. 4 shows the angular distributions to the 3^{+} resonance state of ^{6}Li, for incident neutron energies E_n = 5.74, 7.5, 8.17,10.27, 14.1, 18.0, and 24.0 MeV. We see a good agreement in a wide energy region.

From these results, we can say that the CDCC calculations reproduce the observed inelastic cross sections together with the elastic ones using the same parameter values for λ_v and λ_w. This result indicates that the present CDCC calculations can successfully describe both elastic and inelastic scattering cross sections of *n* - ^{6}Li over somewhat wide energies even lower than 10 MeV.

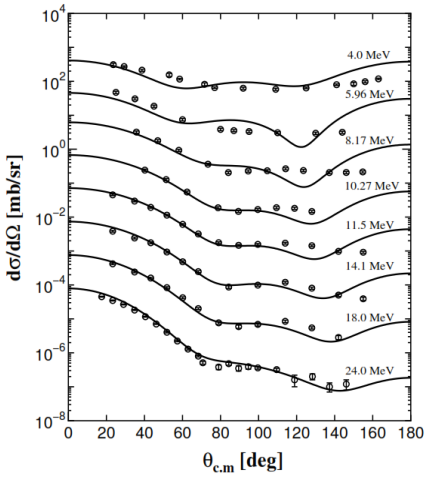

Fig. 3. Elastic angular distribution of the n + ^{6}Li scattering for incident energies between 4.0 and 24.0 MeV. The solid lines and open circles correspond to the calculated results and experimental data [15, 16, 23, 25–28], respectively. The data are subsequently shifted downward by a factor of 10^{-1}–10^{-7} from 5.96 to 24.0 MeV.

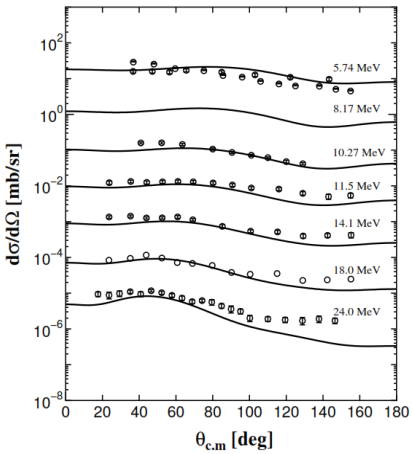

Fig. 4. Angular distributions of the n + ^{6}Li inelastic scattering for the excited 3^+ state at the excitation energy of 2.18 MeV of Li. The solid lines and open circles correspond to the calculated results and experimental data [15, 23, 25, 27–29], respectively. The data are subsequently shifted downward by a factor of 10^{-1}–10^{-6} from 8.17 to 24.0 MeV.

We also analyze the integrated elastic and inelastic scattering cross sections of the n + ^{7}Li scattering at the incident neutron energy region from 1 to 24 MeV, in the same way as the n + ^{6}Li scattering case. Because of the small energy difference (0.478 MeV) between the ground ($3/2^{-}$) and first-excited ($1/2^{-}$) states in ^{7}Li, it is difficult to separate those states in the final state of the n + ^{7}Li scattering experimentally. To compare such experimental data, therefore, we calculate a sum of the cross sections of these two states as the elastic one.

Table 4. The normalization factors λ_v and λ_w for real and imaginary parts, respectively, of the n –^{7}Li folding potential.

E_n (MeV)	λ_v	λ_w	E_n (MeV)	λ_v	λ_w
1.0	1.155	0.0	6.0	1.060	0.0
1.2	1.160	0.0	7.0	1.040	0.0
2.0	1.165	0.0	8.0	1.040	0.0
2.3	1.165	0.0	9.0	1.040	0.0
3.0	1.165	0.0	10.0	1.040	0.0
4.0	1.150	0.0	11.5	1.000	0.1
5.0	1.120	0.0	≥14.1	1.000	0.2

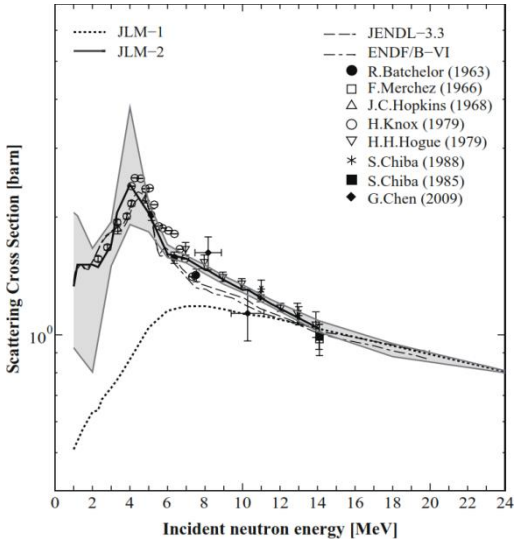

Fig. 5. The integrated elastic n + ^{7}Li scattering cross sections, in comparison with the evaluated data [14,30] and experimental data [15,16,20–23,27,29].

For the n + ^{7}Li elastic scattering of the neutron incident energies from 1 to 24 MeV, we take the normalization factors λ_v =1.0 and λ_w=0.2. The calculated elastic cross sections are presented by the dotted line (JLM-1) in Fig. 5. The imaginary potential is very small as well as the n + ^{6}Li case, and the calculated result shows a good agreement with the evaluated data JENDL-3.3 [14] and ENDF/B-VI [30] in the energy region higher than 14.1 MeV where there are no experimental data. However, the calculated one below 11.5 MeV falls off much faster than the experimental data [15, 16, 20–23, 27, 29]. In the same way as the n + ^{6}Li scattering, we adjust normalization factor λ_v at each incident energy below E_n = 11.5 MeV assuming λ_w = 0. The obtained values of λ_v and λ_w are presented in Table IV including those for E_n ≥14.1MeV, and calculated elastic cross sections are shown by the solid line (JLM-2) in Fig. 5. Values of λ_v are slightly larger than 1.0, and their energy dependence is considered to be owing to formation of compound states of n + ^{7}Li as was discussed the n + ^{6}Li case. It is also seen that the integrated elastic cross section is very sensitive to values of λ_v in lower energies shown by the grey area bounded by upper and lower lines calculated for λ_v±0.01.

Although the above elastic cross section includes the first excited state of ^{7}Li in addition to the ground state, there are many experiments which have measured the γ -ray production cross sections for 478-keV ($1/2^- \rightarrow 3/2^-_{g.s.}$) transition in ^{7}Li following inelastic neutron scatterings. Recently, Nyman et *al.* [8] reported the new data comparing with previous observations. However, there is no theoretical calculation so far. In our CDCC framework with the n − ^{7}Li folding potential fitted to the elastic cross section, it is easy to calculate the inelastic cross section for the first excited $1/2^-$ state at 478 keV with two kinds of the parameter set (JLM-1 and JLM-2). The results are shown in Fig. 6 and compared with experimental data including the recent new data [8]. The JLM-1 calculation is an underestimation and shows the fall-off behavior in the energy region lower than 7 MeV, but the JLM-2 calculation successfully reproduces the experimental data increasing in the low energy region. Especially the peak of cross section around 4 MeV is well explained by the JLM-2 calculation. However, the JLM-2 calculation falling down rapidly cannot reproduce another peak at low energies. Figure 7 we calculate the other integrated inelastic cross section for the 4.65-MeV ($7/2^-$) state of ^{7}Li. In the neutron incident energies from 8 to 14 MeV, we see two groups of experimental data [15–23, 25, 27, 29]; one group is almost flat but another one increases with decreasing of the energy. The evaluation data are also

separated into two groups: The JENDL-3.3 [14] supports the former data but the ENDF/B-VI [30] suggests the latter behavior. Our calculations of the JLM-2 show the consistency with the latter data, although the JLM-1 calculation falls off rapidly as the energy decreases. Using the JLM-2 parameters, we calculate the angular distributions of the elastic cross section where the inelastic ones to the first excited state are included as well. The obtained results are presented in Fig. 8 together with the experimental data for the incident energies from 2.3 to 24.0 MeV [15,23,27–29]. The calculated results are in reasonable agreement with the experimental data. For the inelastic scattering to the $7/2^-$ resonant state of ^{7}Li, Fig. 9 shows the angular distributions of energies from E_n = 8.17 to 24 MeV. Here we calculate differential cross sections of the inelastic scattering for the $7/2^-$ resonant state by taking a sum of the breakup cross section to five discretized $7/2^-$ solutions obtained around the resonance energy. From Fig. 9, we can see that the CDCC calculation with the JLM-2 can also reproduce the inelastic observed cross sections together with the elastic ones.

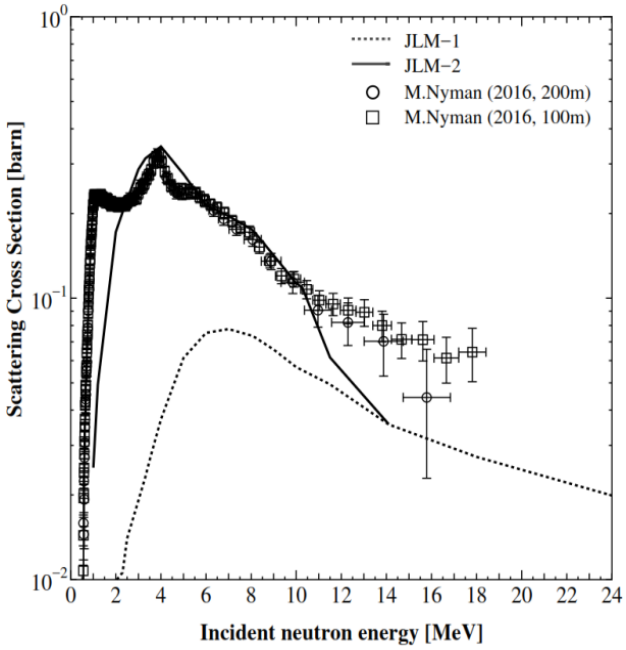

Fig. 6. The integrated inelastic n + ^{7}Li scattering cross sections for the excited $1/2^-$ state at the excitation energy 478 keV of ^{7}Li with experimental data [8].

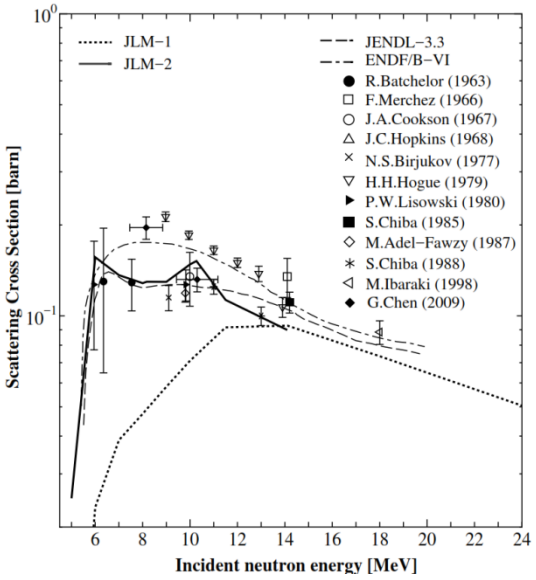

Fig. 7. The integrated inelastic n + ^{7}Li scattering cross sections for the excited 7/2^{-} state at the excitation energy of 4.65 MeV of ^{7}Li, in comparison with the evaluated data [14, 30] and experimental data [15–23, 25, 27, 29].

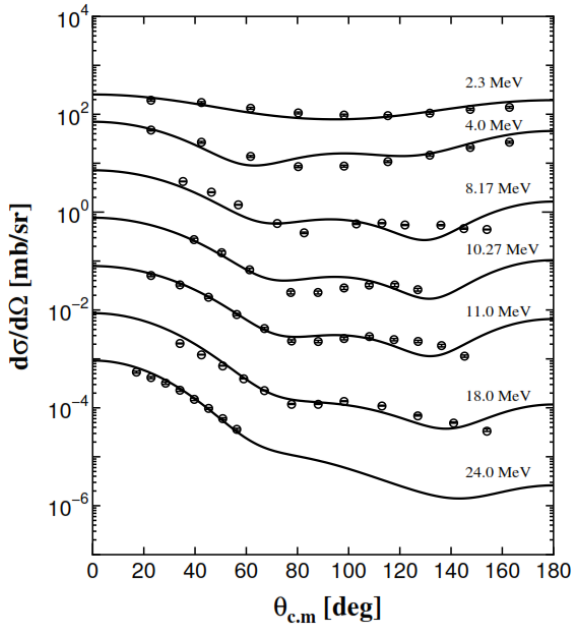

Fig. 8. Elastic angular distribution of the n + ^{7}Li scattering for incident energies between 2.3 and 24.0 MeV. The solid lines and open circles correspond to the calculated results and experimental data [15, 23, 27–29], respectively. The data are subsequently shifted downward by a factor of 10^{-1}–10^{-6} from 4.0 to 24.0 MeV.

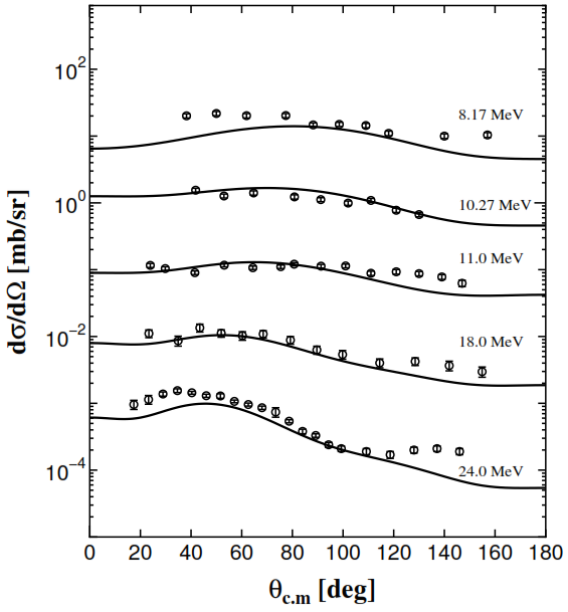

Fig. 9. Angular distributions of the n + ^{7}Li inelastic scattering for the excited 7/2− state at the excitation energy of 4.65 MeV of ^{7}Li. The solid lines and open circles correspond to the calculated results and experimental data [15, 23, 27, 28], respectively. The data are subsequently shifted downward by a factor of 10^{-1}–10^{-4} from 10.27 to 24.0 MeV.

4. Summary

Using the CDCC framework of the *n* + (α+ *d*) and *n* + (α+ *t*) models, we investigated the integrated elastic and inelastic scattering cross sections for ^{6,7}Li at incident neutron energies from 1 to 24 MeV using the *n* + ^{6,7}Li folding potentials with two kinds of the complex-JLM effective nucleon-nucleon interactions [5,7] for higher and lower energy regions. We introduce the normalization factors for real and imaginary parts of these folding potentials comparing with the observed elastic cross sections of the *n* + ^{6,7}Li scattering. The energy independent (JLM-1) and dependent (JLM-2) normalization factors are examined for integrated elastic and inelastic cross sections and angular distributions.

The JLM-2 calculations, in which the energy-dependent normalization factors are determined so as to reproduce the elastic cross section of the whole energy region from 1 to 24 MeV, show a satisfactorily good agreement with the experimental data of inelastic cross sections and angular distributions. From these results, it is concluded

that the CDCC calculations of JLM-2 can explain the experimental data of the integrated inelastic cross sections and angular distributions for the n + ^{6,7}Li scattering cross sections consistently with the integrated elastic cross sections. The application of the CDCC to the low-energy scattering is still an open problem, because assumptions of the CDCC may be too simple for low energy scattering. In the CDCC calculations, rearrangement channels and the antisymmetriztion between nucleons in projectile and target nuclei are neglected. Furthermore, the interaction between incident neutron and target nucleus is not included in the present calculation. For these problems, we here tried to investigate the low energy scattering of n + ^{6,7}Li by introducing a single parameter of the normalization factor for the folding potential based on the effective nucleon-nucleon interaction (JLM). The successful results of the present approach are very promising for more detailed studies of the CDCC in the low energy scattering.

Applying the CDCC framework to the ^{7}Li(α+t)+n model, we investigated the integrated neutron elastic and inelastic scattering cross sections for the ^{7}Li target at incident neutron energies below 14.1 MeV using the cluster-folding of the optical model potentials and above 14.1 MeV using the JLM single-folding potential. Energy dependence of the normalization factors, λ_{v} and λ_{w}, of the cluster folding potential is introduced and determined from measured integrated elastic cross sections. The CDCC calculation gives a satisfactorily good agreement with the experimental data.

Acknowledgements

We would like to thank the members of the nuclear theory group at Hokkaido University and Dr. Markus Nyman and his experimental group of Institute for Reference Materials and Measurements, Belgium. This work was supported by "R&D Platform Formation of Nuclear Reaction Data in Asian Countries (2010–2013)," Asia-Africa Science Platform Program, and Grant-in-Aid for Publication of Scientific Research Results (Grant No. 257005), Japan Society for the Promotion of Science. M.A. and K.K. also thank the International Collaboration of the Al-Farabi Kazakh National University (Grants No. 3106/GF4 and No. 1550/GF3) for support.

References

[1]. T. Matsumoto, D. Ichinkhorloo, Y. Hirabayashi, K. Katō, and S.Chiba, Phys. Rev. C**83**, 064611(R) (2011).

[2]. D. Ichinkhorloo, Y. Hirabayashi, K. Katō, T. Matsumoto, and S.Chiba, J. Nucl. Sci.Technol. **48**, 1357 (2011).

[3]. D. Ichinkhorloo, Y. Hirabayashi, K. Katō, M. Aikawa, T.Matsumoto, and S. Chiba, Phys. Rev. C **86**, 064604(R) (2012).

[4]. M. Kamimura, M. Yahiro, Y. Iseri, Y. Sakuragi, H. Kameyama, and M. Kawai, Prog. Theor. Phys. Suppl. **89**, 1 (1986); Y.Sakuragi, M. Yahiro, and M. Kamimura, Prog. Theor. Phys.**89**, 136 (1986).

[5]. J.-P. Jeukenne, A. Lejeune, and C. Mahaux, Phys. Rev. C **16**, 80 (1977).

[6]. H. Guo, Y. Watanabe, T. Matsumoto, K. Ogata, and M. Yahiro, Phys. Rev. C **87**, 024610 (2013).

[7]. A. Lejeune, Phys. Rev. C **21**, 1107 (1980).

[8]. M. Nyman, F. Belloni, D. Ichinkhorloo, E. Pirovano, A. J. M.Plompen, and C. Rouki, Phys. Rev. C **93**, 024610 (2016).

[9]. S. Saito, Prog. Theor. Phys. Suppl. **62**, 11 (1977).

[10]. E. Hiyama, Y. Kino, and M. Kamimura, Prog. Part. Nucl. Phys.**51**, 223 (2003).

[11]. A.M.Moro, J.M. Arias, J. Gomez-Camacho, I. Martel, F. Perez-Bernal, R. Crespo, and F. Nunes, Phys. Rev. C **65**, 011602(R) (2001).

[12]. T. Matsumoto, T. Kamizato, K. Ogata, Y. Iseri, E. Hiyama, M.Kamimura, and M. Yahiro, Phys. Rev. C **68**, 064607 (2003).

[13]. T. Egami, K. Ogata, T. Matsumoto, Y. Iseri, M. Kamimura, and M. Yahiro, Phys. Rev. C **70**, 047604 (2004).

[14]. K. Shibata, T. Kawano, T. Nakagawa, O. Iwamoto, J. Katakura, T. Fukahori, S. Chiba, A. Hasegawa, T. Murata, H. Matsunobu, T. Ohsawa, Y. Nakajima, T.

Yoshida, A. Zukeran, M. Kawai, M. Baba, M. Ishikawa, T. Asami, T. Watanabe, Y. Watanabe, M. Igashira, N. Yamamuro, H. Kitazawa, N. Yamano, and H. Takano, Japanese Evaluated Nuclear Data, Library Version 3 Revision-3: JENDL-3.3, J. Nucl. Sci. Technol. **39**, 1125 (2002).

[15]. G. Chen, X. Ruan, Z. Zhou, J. Zhang, B. Qi, X. Li, H. Huang, H. Tang, Q. Zhong, J. Jiang, B. Xin, J. Bao, and L. Chen, Nucl. Sci. Eng. **163**, 272 (2009).

[16]. H. H. Hogue *et al.*, Nucl. Sci. Eng. **69**, 22 (1979).

[17]. P. W. Lisowski *et al.*, Report No. LA-8342 (Los Alamos Scientific Laboratory, Los Alamos, 1980).

[18]. J. A. Cookson *et al.*, J. Nucl. Phys. A **91**, 273 (1967).

[19]. M. Adel-Fawzy *et al.*, Nucl. Instrum. Methods **169**, 533 (1980).

[20]. R. Batchelor *et al.*, J. Nucl. Phys. **47**, 385 (1963).

[21]. J. C. Hopkins *et al.*, J. Nucl. Phys. A **107**, 139 (1968).

[22]. F. Merchez *et al.*, J. Phys. Colloque **27**, 1, 61 (1966).

[23]. S. Chiba *et al.*, J. Nucl. Sci. Technol. **25**, 2, 210 (1985).

[24]. N. S. Biryukov, B. V. Zhuravlev, N. V. Kornilov, V. I. Popov, P. Rudenko, O.A.Salnikov, and V. I. Trykova, At. Energ. **43**, 1787 (1977).

[25]. M. Ibaraki *et al.*, JAERI-Research Report No. 98-032 (Japan Atomic Energy Research Institute, Ibaraki, 1998).

[26]. B. Smith *et al.*, Nucl. Phys. A **373**, 305 (1982).

[27]. S. Chiba, M. Baba, N. Yabuta, T. Kikuchi, M. Ishikawa, N. Hirakawa, and K. Sugiyama, in *Proceedings of the International Conference on Nuclear Data for Science and Technology* (Mito, 1988), p. 253.

[28]. L. F. Hansen, J. Rapaport, X. Wang, F. A. Barrios, F. Petrovich, W. Carpenter, and M. J. Threapleton, Phys. Rev. C **38**, 525 (1988).

[29]. H. Knox and R. O. Lane, J. BAP **23**, 942(DC2), 7811.

[30]. Cross Section Evaluation Working Group, ENDF/B-VI Summary Documentation, Report BNL-NCS-17541 (ENDF-201) (Brookhaven National Laboratory, Upton, 1991).

A new Java-based EXFOR editor

A. Sarsembayeva[1,*], S. Ebata[1], M. Chiba[2], N. Otuka[3], M. Aikawa[1]

[1]*Faculty of Science, Hokkaido University, Sapporo 060-0810, Japan*
[2]*Sapporo-Gakuin University, Ebetsu, 069-8555, Japan*
[3]*Nuclear Data Section, International Atomic Energy Agency, A-1400 Wien, Austria*

Abstract. The EXFOR database contains the largest collection of experimental nuclear reaction data. Nuclear data, encompass quantitative results of nuclear physics research and comprise the areas of nuclear reaction, nuclear structure and nuclear decay data. Nuclear data have been utilized in the following many areas: nuclear physics, astrophysics, nuclear engineering, medicine, etc. To keep the nuclear reaction database high quality for such users, an editor to compile the data plays an important role. In this report, we present a new EXFOR editor system based on the Java programming language. The aim of a new editor currently being developed by the Hokkaido University Nuclear Reaction Data Centre (JCPRG, formerly Japan Charged-Particle Nuclear Reaction Data Group) is to provide an easy-in-use environment to EXFOR compilers. The latest features added in the ForEX editor are described.

1. Introduction

Nuclear data are quantitative results of scientific investigations of the nuclear properties of matter. Examples of nuclear data include cross sections, half-lives, decay modes and decay radiation properties. By compiling nuclear data we can support various applications, assist scientific discoveries and preserve the knowledge for future generations. Applications of nuclear data include all areas of nuclear science and technology, covering energy applications [1]:

- fission reactor design,
- nuclear fuel cycles,
- nuclear safety,

- reactor monitoring,
- waste disposal and transmutation.

There are also many nuclear applications outside the field of fission reactor technology:

- cancer radiotherapy,
- production of radioisotopes for medical and industrial applications,
- accelerator shield design,
- personnel dosimetry and radiation safety.

The Nuclear Data Section (NDS) of the International Atomic Energy Agency (IAEA) [2] provides nuclear data services to scientists on a worldwide scale with particular emphasis on developing countries. The EXFOR database [3] includes neutron-induced, charged-particle-induced and photon-induced reaction data. The EXFOR library is the most comprehensive collection of experimental nuclear data available. The availability of compilations that provide an easy access to nuclear data is an essential tool for experimenters and scientists. The following tools helps us to compile and visualize the nuclear data:

- Editing system:
  - Web-based editor
  - Stand-alone type editor
- Checking tools
- Graph digitizer

With the aim to meet requirements of EXFOR compilers, Nuclear Reaction Data Centre (JCPRG) [4] indicated that steps be taken on the issue of editor update. We learned that the only way for compilation to consistently succeed today is to attract new nuclear data compilers by creating them an easy-in-use editor. This has been the key motivation for the development of an advanced EXFOR editor system. The developing editor, called ForEX (**For EX**FOR) [5] would address the growing needs

of traditional EXFOR compilers.

2. Method

In order to establish an OS independent EXFOR editor system, Java was selected as a programming language for ForEX. The main window of ForEX editor is divided into four sections (Fig. 1). The menu bar at the top is used to perform common operations, which includes the ‘File’ and ‘Edit’ menus. Under the menu bar, three very frequently used controls are provided: ‘DANLO’ for extraction of the new dictionaries from the backup dictionary file, ‘CHEX’ for checking of EXFOR entries created by compiler. The ‘OPEN’ button allows the compiler to load the entry file with a ‘.ser’ extension. Using the ‘EDIT’ button we can reedit the serialized files. The main task of the ‘EXFOR’ button is to get EXFOR output format. The left panel is used to display the content menu, which consists input forms for bibliography and information commonly applied to all data sets of the EXFOR entry (Subentry 1). The right section of the window is used to input experimental nuclear data.

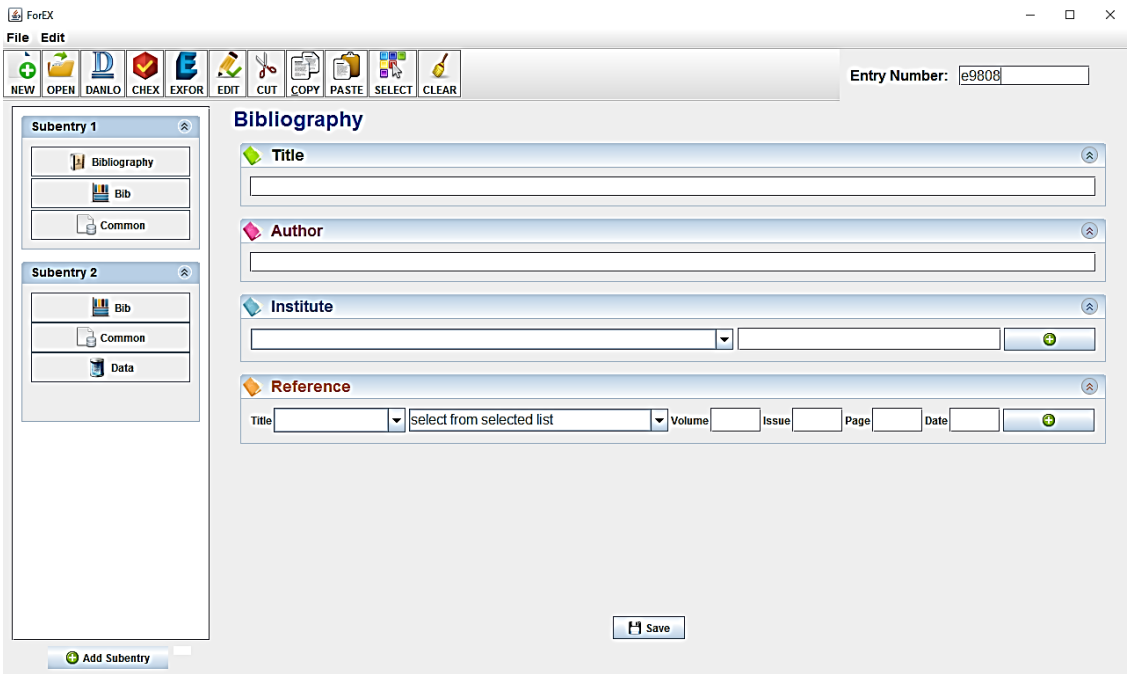

Fig. 1. The layout of main window of the ForEX.

3. Result & Discussion

The efficiency of compilation work directly depends on well-designed content and its functionality. The new EXFOR editor system was developed using Java language. The primary motivation was the need for a platform-independent language that could be accessible in various operation systems. The primary purpose of ForEX is to provide advanced functionality for the compilation of experimental nuclear reaction data. ForEX was designed for both novice and expert users to allow compilers to save the compilation time by using advanced features of the editor. During the development of new EXFOR editor we followed 3 key principles:

- Intuitive (no need to invest time into learning):
  - ✓ You shouldn't have to read a manual to become more productive;
  - ✓ Knowledge of EXFOR format is not required.
- Simplicity (the quality of being easy to understand):
  - ✓ The Toolbar is the most important design element on an editor development because it is a singular tool that gives users a sense of orientation;
  - ✓ Clean and intuitive user-interface.
- User-friendliness (the quality of being functional):
  - ✓ Collapsible/expandable item;
  - ✓ Add/remove buttons;
  - ✓ Filterable suggestion field;
  - ✓ Text filtering for a table;
  - ✓ Dynamic suggestion field;
  - ✓ Nuclide field.

As we aimed to create an easy-in-use environment for EXFOR compilers, described above advanced components gives a great opportunity to compilers to

achieve easiness and efficiency during the compilation time.

The advanced functionalities presently used to achieve the user-friendliness are briefly described below (for more details, see [6]).

- Collapsible/expandable item

  Collapsible/expandable function was implemented to simplify the tasks and decisions by creating a visual representation of a user interface. This function can reduce complexity for users.

- Add/remove buttons

  Similar to the concept of collapsible/expandable items, the number of input areas must be minimum at first. These areas can be added/removed interactively by buttons.

- Filterable suggestion field

  Filterable suggestion field aims to save compilation time and allows to compilers to avoid the mistakes.

- Text filtering for a table

  Similar to the concept of filterable suggestion fields, codes can be suggested by a keyword input. With the help of text filtering, an appropriate list of reaction codes can be obtained easily.

- Dynamic suggestion field

  The main function of a dynamic suggestion fields is to make data input easier and more reliable. For example, the compiler chooses an input from one list, which restricts the related contents of another list.

- Nuclide field

  Nuclide field accept 20 types of different keywords with a same final output.

The program consists of external tools such as DANLO and CHEX. When a DANLO button is clicked, the FileChooser dialog box is shown. This allows extraction of the dictionaries-backup file (DAN_BACK_NEW.XXXX) in appropriate

user directory. The CHEX program is used to check EXFOR entries. The details of the extraction of dictionaries are described in Reference 7.

ForEX provides a mechanism, called data file serialization where the serialized files represented as a sequence of bytes that includes the data stored in the file. After a serialized data has been written into a file with a '.ser' extension, it can be read from the file and deserialized. Most impressive is that the entire process is JVM independent, meaning the data can be serialized on one platform and deserialized on an entirely different platform.

4. Conclusions

Motivated by the platform independent features of Java, the JCPRG developed a new Java-based EXFOR editor for data compilation. The developed editor, ForEX would address the growing needs of traditional EXFOR compilers as well as advanced functionalities. As aforementioned, ForEX was developed by following 3 principles: intuitive, simplicity and user-friendliness. The combination of these 3 principles contributes to improving the usability. Advanced features implemented in the program can allow compilers to save time and avoid mistakes.

At the present time debugging and testing EXFOR output files are in progress. Execution of the program was only tested in Windows and Linux. Testing on the Mac OS is in progress.

References

[1] Nuclear Data Services. Available from: https://www-nds.iaea.org/

[2] N. Otuka (ed.), Report INDC(NDS)-0401 Rev.6, International Atomic Energy Agency (2014).

[3] EXFOR Database. Available from: https://www-nds.iaea.org/exfor/exfor.htm

[4] Nuclear Reaction Data Centre. Available from: http://www.jcprg.org/

[5] A. Sarsembayeva et al.: Proceedings of the Sixth Workshop on Asian Nuclear Reaction Database Development. Hokkaido University, Sapporo, Japan, 15-17

September 2015. P.39.

[6] A. Sarsembayeva et al.: Proceedings of the 2015 Symposium on Nuclear Data. Ibaraki Quantum Beam Research Center, Tokai-mura, Ibaraki, Japan, 19-20 November, 2015. P.81

[7] A. Sarsembayeva et al.: Report on the status of IT environment. JCPRG Annual Report No.5 (2015). P.26.

Investigation of activation cross-sections of alpha-induced nuclear reactions on natural silver

Kwangsoo Kim[a], Muhammad Shahid[a],, Haladhara Naik[a,b], Muhammad Zaman[a], Guinyun Kim[a*]

[a] *Department of Physics, Kyungpook National University, Daegu 702-701, Republic of Korea*

|[b] *Radiochemistry Division, Bhabha Atomic Research Centre, Mumbai 400085, India*

*Corresponding author: gnkim@knu.ac.kr

Abstract. The excitation functions of ^{108m,108g,109g,110m,110g,111g}In, ^{109g,111m}Cd and ^{105g,106m,110m,111g}Ag from alpha-induced reactions on ^{nat}Ag were measured from their respective threshold to 45 MeV by using a stacked-foil activation technique at the MC-50 cyclotron of the Korean Institute of Radiological and Medical Sciences. The results were compared with the earlier reported data as well as with the theoretical values obtained from the TENDL-2013 library based on the TALYS 1.6 code. Our measurements in the energy region from the threshold energy to 45 MeV are in general good agreement with the other experimental data and calculated results. The integral yields for thick target of the produced radionuclides were also deduced from their measured cross sections and the stopping power of natural Silver. The measured excitation functions find importance in various practical applications including nuclear medicine and improvement of nuclear model calculations.

Measurement and EXFOR compilation of the neutron-induced activation cross sections in the energy range up to 20 MeV

V. Semkova

Nuclear Data Section, International Atomic Energy Agency, Vienna, Austria

Neutron-induced reaction cross sections are important for many fields of science and applications. The analyses of the radioactivity induced at various nuclear installations require nuclear reaction cross sections and decay data for all comprising target nuclides. The material damage is largely governed by the helium and hydrogen production. The radiation hazards and decay heat are associated with the decay of the activation products. The neutron transport depends on the (in)elastic scattering and (n,xn) cross sections. The experimental data are important for the testing and development of nuclear reaction models.

Activation technique is a powerful method to study nuclear reaction cross sections providing radioactive decay of the reaction products. Depending on the decay scheme, cross sections for the production of the particular excitation level can be determined as well. Such data are of considerable significance for the development of the nuclear models, since the isomeric state population is more difficult to predict than those for the total reaction cross sections [1]. The magnitude and the energy dependence of the isomeric cross section ratio $\sigma_m/(\sigma_m + \sigma_g)$ depend on the decay scheme, properties of the nuclear levels involved and branching ratios. So, proper reporting and EXFOR compilation of the ground state, isomeric and total cross sections ensure consistency and comparability of the results obtained from different experiments. To account for the specific level of the reaction product isomeric flags –G, –M(i) and –L(i) are provided in the EXFOR compilation rules. For the partial contribution or exclusion of the decay of the higher energy levels to the measured state M+ or M- are codded in the sub-field 5 (SF5) of the reaction quantity code REACTION. So, in cace of existance of one or more metastable states, the decay

scheme need to be taken into accound in order to determine properly the measured cross section.

The decay characteristics of the Co-58 ground and 24.889 keV metastable states are presented on Fig. 1 [2]. Based on the measured ^{58}Ni(n,p) isomeric cross section ratio (Fig. 2), compiled in EXFOR database [3], one can conclude that the ^{58}Ni(n,p)^{58m}Co cross section is increasing form 30 to around 50% of the total cross section in the energy range from 1 to 20 MeV and respectively the ground state cross section is decreasing from 70 to 50%.

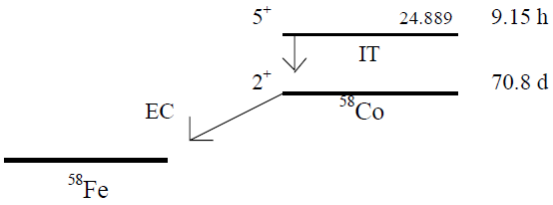

Fig 1. Decay characteristics of the ^{58}Co ground and 25 keV metastable states (IT=100%).

However the plot of the ^{58}Ni(n,p) total, ground state and metastable state cross sections (Fig. 3) [4] shows that some of the compiled ground state cross sections are of the same order of magnitude as the total cross section data. The publications and the EXFOR compilations have been checked in order to clarify the inconsistency. In some cases authors incorrectly have reported total as a ground state cross section or do not provide sufficient information for the measurement procedure, which in this particular case require analysis of the ground state activity as a function of time after end of irradiation in order to determine the ground state cross section. Some mistakes in EXFOR compilation were identified as well. For example, in the compilation of Journal of the Physical Society of Japan, Vol.17, p.1215 (1962) the results are compiled as a ground state cross section although the authors have stated that the data were measured after the metastable state decay completely to the ground state. The ground state cross sections data that have been provided with sufficient experimental information are compared with the total cross section data on Fig. 4. There is clear

separation of the ground state cross sections from the bulk of the total cross sections for those data.

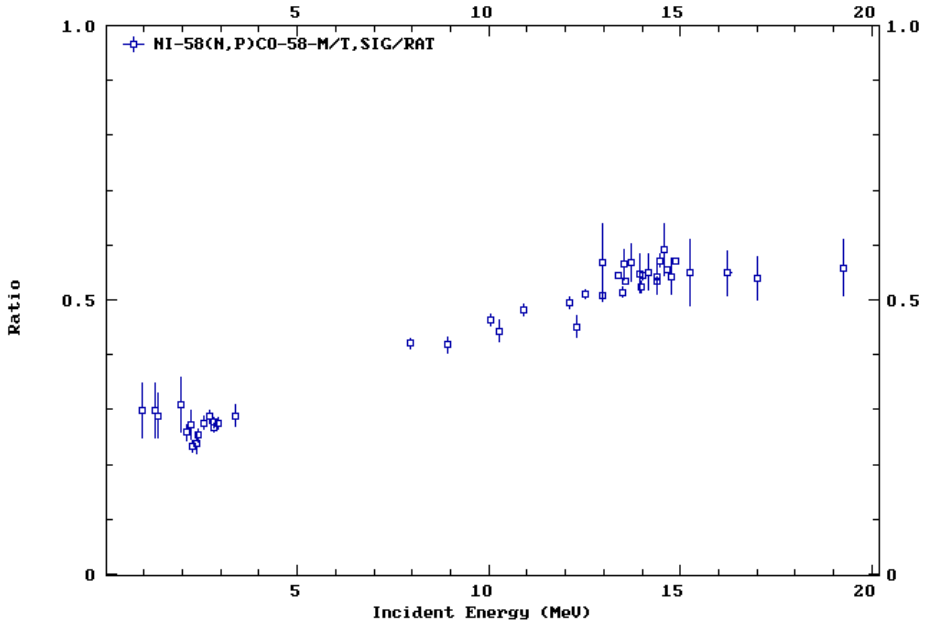

Fig. 2. ^{58}Ni(n,p) meta to total cross section ratio compiled in EXFOR.

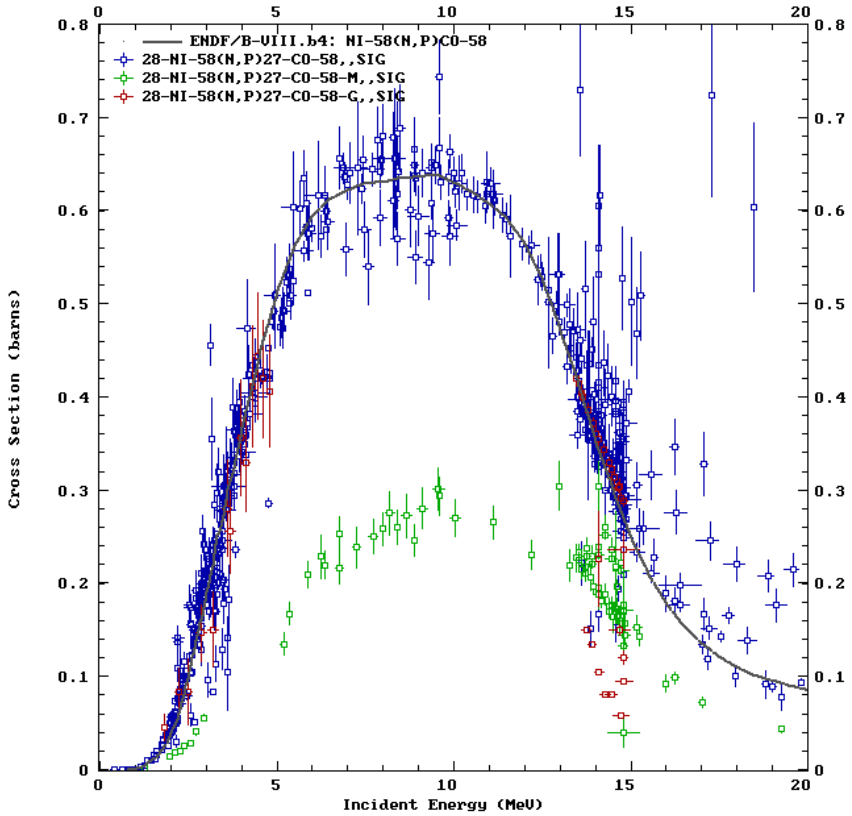

Fig. 3. ^{58}Ni(n,p) isomeric ground state and total cross sections compiled in EXFOR.

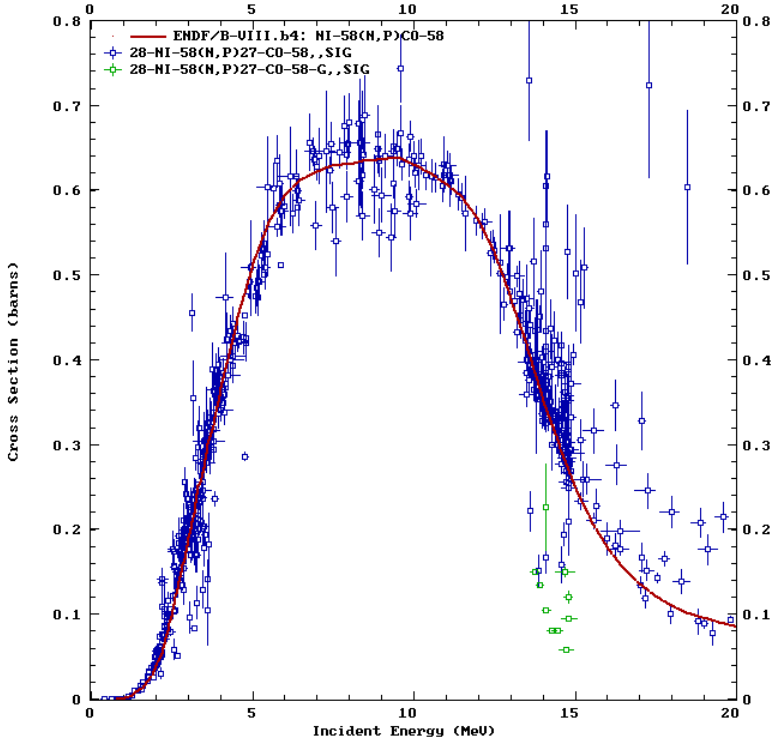

Fig. 4. ^{58}Ni(n,p) total cross sections and selected ground state cross section data.

In conclusion, if there exist one or more metastable states decaying through isomeric transitions to the lower energy levels, a proper assignment of the of the measured cross section as well as a description of the applied experimental procedure is required since both the magnitude and the trend as the function of the incident energy depend strongly of the incident projectile and the properties of the nuclear levels involved.

References

[1] S. Sudar et al., Phys. Rev. C **53**, 2885 (1996)

[2] Caroline D. Nesaraja et al., Nucl. Data Sheets, **111**, 897-1092 (2010)

[3] N. Otuka et al., Nucl. Data Sheets, **120**, 272–276 (2014)

[4] IAEA Nuclear Data Services: http://www-nds.iaea.org/ .

Recent EXFOR compilation in CNDC

Chen Guochang, Wang Jimin, Tao Xi, Zhuang Youxiang, Ge Zhigang

China Nuclear Data Center, China Institute of Atomic Energy, Beijing, China, 102413

1. Introduction

The EXFOR library has become the most comprehensive compilation of microscopic experimental nuclear reaction data. It contains cross sections and other nuclear reaction quantities induced by neutron, charged-particle and photon beams, etc. Currently compilation is mandatory for all low and intermediate energy neutron and light charged-particle induced reaction data. Heavy-ion and photon induced reaction data are also additionally compiled on a voluntary basis.

Currently fourteen data centers are participating in the International Network of Nuclear Reaction Data Centres (NRDC) and are collaborating mainly for compilation and exchange of experimental data by using the common Exchange Format (EXFOR Format) under the auspices of the IAEA Nuclear Data Section (NDS).

2. EXFOR compilation in CNDC

Since China joined IAEA at 1984 and China Nuclear Data Center (CNDC) joined NRDC in 1987, we are takes part in scanning Chinese journals and compiling EXFOR entries and collaborating with NRDC. CNDC is one specialized center at NRDC as shown in **Fig. 1**. Which the experiments are carried out by Chinese researcher, the experiments are measured in China and measurements are published in Chinese journals, compilation of bibliographic references (CINDA) to microscopic neutron reaction data and related data published in Chinese, CNDC need to scan and collect measured results and compile these data and information as EXFOR format including neutron and charge particle induced reactions. CNDC are respond more than 9 Chinese journals now such as **Fig. 2** and IAEA assigns EXFOR compilation task.

Country	Center	Joined
Russia	Nucl. Struc. & Nucl. Reac. Data Centre	1974
Japan	Japan Nuclear Reaction Data Center	1975
Russia	Centre for Exp. Photonuclear Data	1982
China	*China Nuclear Data Center*	*1987*
Japan	Nuclear Data Center	1991
Korea	Nuclear Data Evaluation Laboratory	2000
India	Nuclear Data Section	2008

Fig. 1. The specialized center at NRDC.

In 1985, IAEA and CNDC hold a working meeting about compilation in EXFOR. Fifteen charged particle EXFOR entries were transmitted to IAEA for NRDC communication at this meeting as shown in **Fig. 3** and started to compile neutron entries at 1989.

1. Chinese Physics C(ENG/2007;HEN)
2. Atom. Energy Sci. & Tech.(CHN/1959)
3. J. of Nucl. & Radiochemistry(CHN/1979)
4. Nuclear Physics Review(CHN/1984)
5. Nuclear Techniques(CHN/1978;+ENG/1989)
6. Com. of Nucl. Data Prog.(ENG/1989)
7. Nuclear Science and Techniques(ENG/1989)
8. Chinese Physics Letters(ENG/1984)
9. Chinese Physics B (ENG)
10. Acta Physica Sinica(ENG/1933)
11. Conference, Workshop etc.

Fig. 2. List of the responsibility of CNDC.

01 Li Zhichang+ Yuanzineng Kexue Jishu 3(1977)229
02 Liang Qichang+ Yuanzineng Kexue Jishu 1(1977)10
03 Mao Zhenlin+ Conf. on Low Energy Nucl. Phys.3(1972)
04 Yuan Rongfang+ Chin. J. Nucl. Phys. 3(1981)155
05 Jiang Chenglie+ Conf. on Low Energy Nucl. Phys.3(1972)
06 Sun Hancheng+ Yuanzineng Kexue Jishu 3(1984)329
07 Yan Chen+ Chin. J. Nucl. Phys. 2(1980)137
08 Sun Hancheng+ Yuanzineng Kexue Jishu 2(1981)185
09 Ma Weiyi+ Chin. J. Nucl. Phys. 2(1980)239
10 Shen Wenqen+ High Energ.Phys.Nucl.Phys.1(1977)70
11 Tao Zhenlan+ Canadian Nucl Technol.45(1987)
12 X.Long+ NST-001 (1985)
13 Long Xianguan+ NST-003 (1989)
14 Tao Zhenlan+ Chin. J. Nucl. Phys. 3(1981)242
15 Tao Zhenlan+ Yuanzineng Kexue Jishu 5(1983)506

Fig. 3. CNDC provided the first 15 charged particle EXFOR entries.

	No.	Ref.	Title	Vol.	Issue	Page	Lab	Publish date	Author	Status	Action	Delay date(m)	Compiler	Entry	Sub	Memo
修改 详情	1	J,NCA	Cross section measurements for gallium in the neutron energy range of 13.5 to 14.8 MeV	100	4	231	3CPRMUV	201202	J.Luo	Allocated	Compiling	6	Youxiang ZHUANG	32704	n	Assigned this entry a ···
修改 详情	2	J,IPC	Cross-sections for formation of 99mTc through nat-Zn(n, x)99mTc reaction induced by neutrons at 13.5 and 14.8 MeV	81	5	495	3CPRMUV	201201	Junhua Luo	Allocated	Compiling	7	Youxiang ZHUANG	32702	n	Assign this entry is ···
修改 详情	3	J,IPC	Cross-sections for (n,2n), and (n,a) reactions on 59Rh isotope around neutron energy of 14 MeV	81	10	1563	3CPRLNZ	201204	Yanbin Zhang	Allocated	Compiling	4	Jimin WANG	32701	n	Assign this entry is ···
修改 详情	4	J,JNR	Cross section measurements for 141Pr(n, g)142Pr reaction at neutron energies from 13.5 to 14.8 MeV	293	1	261	3CPRMUV	201204	Junhua Luo	Allocated	Compiling	4	Guochang CHEN	32703	n	It is assigned at Aug ···
修改 详情	5	J,NPN	239Pu(nth, f)裂毒命裂变产物产额测量	34	2	88	3CPRAEP	201203	刘祖龙	Allocated	Compiling	5	Guochang CHEN	32700	n	It is assigned at Au ···
修改 详情	6	J,EPJ/A	New determination of the astrophysical 13C(p, γ) 14N S(0) factors and reaction rates via the 13C (7Li, 6He)14N reaction	48	2	13	3CPRAEP	201202	Y.J.Li	Allocated	Compiling	6	Xi TAO	S0054	cp	Assigned this entry ···
修改 详情	7	J,NSR	Cross section measurements for (n,p) reaction on stannum isotopes at neutron energies from 13.5 to 14.8 MeV	35	5	445-448	3CPRLZT	201105	PU Zhongsheng(蒲忠胜)	Allocated	Compiling	15	Youxiang ZHUANG	32699	n	Finish compile at Ju ···
修改 详情	8	ASI	13 光电子伏系统所引起的一些反应的激光函数	22	2	250	3CPRNRS	198602	程晓五	Allocated	Finalized	558	Guochang CHEN	S0060	cp	Finalized this entry ···
修改 详情	9	JP/CS	Fusion-fission and quasi-fission competition in the 32S+184W reaction	282	1	12013	3CPRAEP	201103	K Q Zhang	Allocated	Compiling	17	Youxiang ZHUANG		cp	This is calculation r ···
修改 详情	10	J,EPJ/A	Level structures in the 114In nucleus	47	11	141	3CPRAEP	201111	C B Li			9			cp	This paper couldn't b ···

Fig. 4. EXFOR compilation managed Website.

Present we have a small group to attend EXFOR compilation work. Everyone respond to scan 2 journals, collect the scanning results of all responsible journals, and assign neutron and charged particle tasks. After that, upload the information such as the assigned entry No., paper in pdf, author, publication date, delayed date, the compiler and the processing of compilation to our EXFOR compilation managed Website as shown in **Fig. 4**.

Since 2009, CNDC compiled 152 EXFOR entries as shown in **Fig. 5** which is included 61 neutron and 91 charged particle entries. We can find recently the charged particle induced reaction measurement is become more and more. Up to now, we still have more than 29 entries for checking and correction, and there have more than 8 entries under compilation. And we also remain a lot of charge particle papers in earlier issues of "High Energy Physics and Nuclear Physics" and "Chinese Nuclear Physics" to be compile in the future.

In 2016, we have compiled 41 articles as 34 EXFOR files and sent to NDS for checking and correction, which is included 11 neutron and 24 charge particle or heavy ion induced reactions.

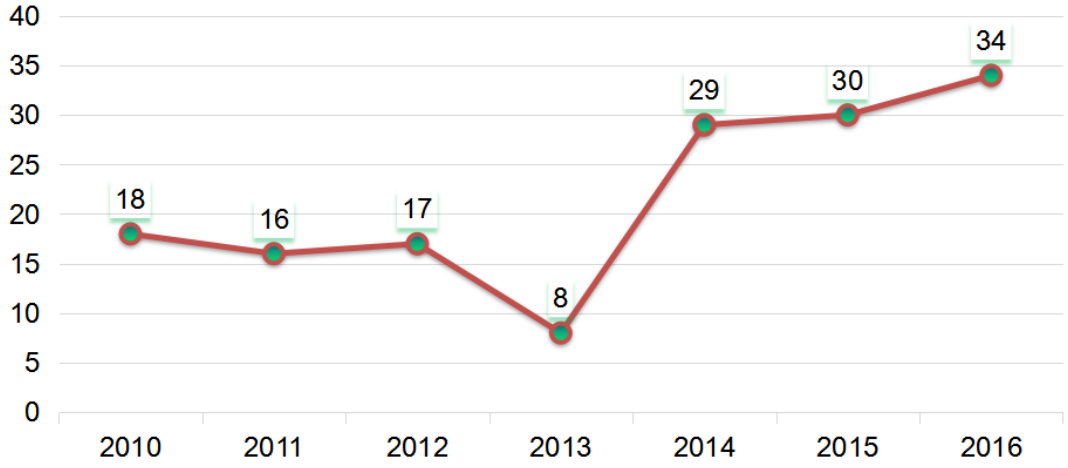

Fig. 5. Compiled EXFOR entries of each year.

3. Nuclear Data Service

CNDC provides the nuclear data service in China for different institute, school or other requirements. CNDC joined the developing of Chinese basic database and established a "The Database of Nuclear Physics" website as shown in **Fig. 6** including experimental data (EXFOR), evaluation data, decay data, nuclear structure, astrophysical data and nuclear data for medical applications for online retrieve and plotting, and the website is "www.nuclear.csdb.cn". CNDC also established the mirror site of IAEA-NDS at Aug. 31 2013, which is "www-nds.ciae.ac.cn". And the database of this mirror site is update with IAEA-NDS website at the same time. Up to now, the contents of mirror site includes EXFOR database and evaluation database as shown in **Fig. 7**. And the contents will be enriched in the future.

Fig. 6. Webpage of "The Database of Nuclear Physics".

Fig. 7. Webpage of IAEA-NDS mirror site.

4. Conclusion

The needs for experimental reaction data are always growing. CNDC response to scan, collect and compile the experimental information which are carried out by Chinese researcher, the experiments are measured in China and measurements are published in Chinese journals, and related data published in Chinese. Present CNDC have a small group to attend EXFOR compilation work and construct an EXFOR compilation managed Website for EXFOR compilation organization. CNDC will continue to scan, collect and compile EXFOR data and collaborate with NRDC.

Theoretical calculations and analysis for n+^{6}Li reaction

Xi Tao, *Jimin* Wang, *Guochang* Chen, and *Qingbiao* Shen

China Nuclear Data Center, China Institute of Atomic Energy, Beijing 102413, China

R-matrix theory is an important theory of light, medium and heavy mass nuclides nuclear reaction in the resonance energy range. FDRR is short for Full and Diagonal Reduced R-matrix. It is a theoretical code, which is based on R-matrix theory and compiled by FORTRAN language. It is developed by the China Nuclear Data Center (CNDC) and Nankai University.

Four R-matrix methods have been compiled in FDRR code. They are MLBW and reduced R-matrix method, diagonal energy shift reduced R-matrix method, full R-matrix method, and un-diagonal energy shift reduced R-matrix method. There are 2 input files for FDRR code, FDRRi.dat and FDRRk.dat files. FDRR code can be used for calculating the cross sections, angular distributions, and polarization Data of 2-bodys reactions.

The cross sections and angular distributions of n+6Li reaction are calculated and analyzed by FDRR code. The process of n+^{6}Li reaction is very complicated. Considering the same residual nucleus, the reaction channels are simplified as Fig.1

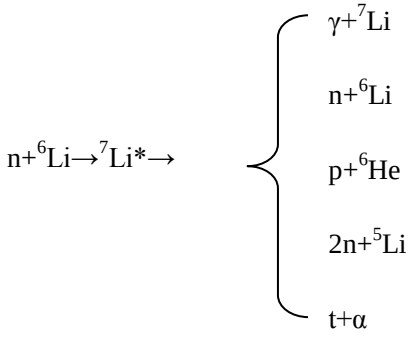

Fig. 1. The reaction process of n+^{6}Li

Assuming that the energy levels are not related, MLBW and reduced R-matrix method is used for calculating n+^{6}Li reaction below 20 MeV.

Fig. 2 shows that the total cross section of n+^{6}Li compared with the experimental data [1-5]. The calculation result is in good agreement with the experimental data from 10 eV to 20 MeV.

Below 0.1 MeV, the calculation of hard sphere scattering agrees with the measure of V. P. Alfimentkov [11]. The result of the resonance peak is also in good agreement with the experimental data [4, 6-11] in Fig. 3.

The shape of ^{6}Li(n,t) cross section is almost the same with the experimental data [12-17]. The peak of the calculation is not very good, and need to be improved.

.

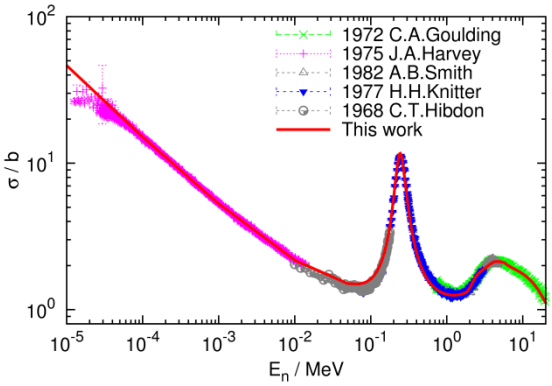

Fig. 2. Total cross section of n+^{6}Li reaction.

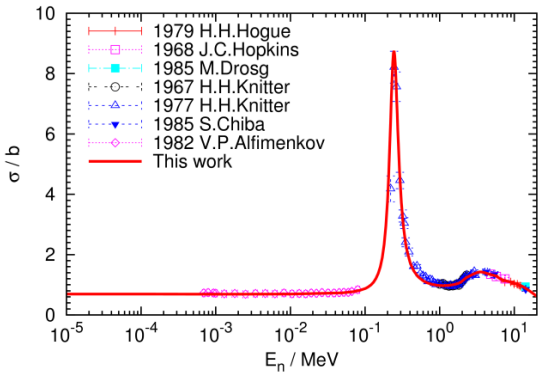

Fig. 3. Elastic scattering cross section of n+^{6}Li.

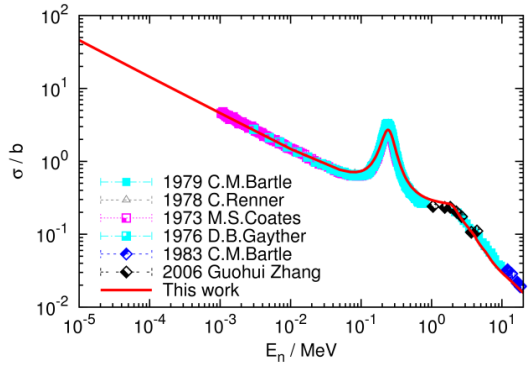

Fig. 4. The cross section of ^{6}Li(n,t) ^{4}He reaction.

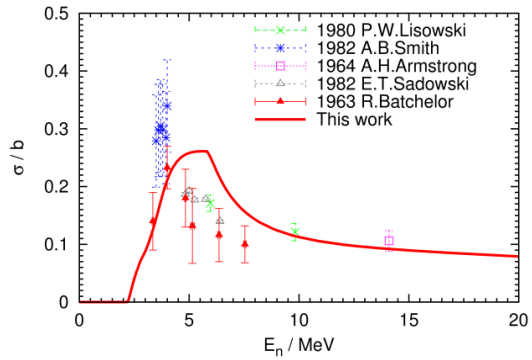

Fig. 5. The cross section of ^{6}Li(n,n$_1$) reaction.

Fig. 5 is the inelastic scattering result of the first excited state. The theoretical calculation is a little higher than experiment data [3, 18-21]. The threshold of ^{6}Li(n,nda) is lower than the first excited energy level, the first excited state is unstable. The accuracy of measurement is not high. The result of the second excited state is shown in Fig. 6, which is in good agreement with experimental data [22].

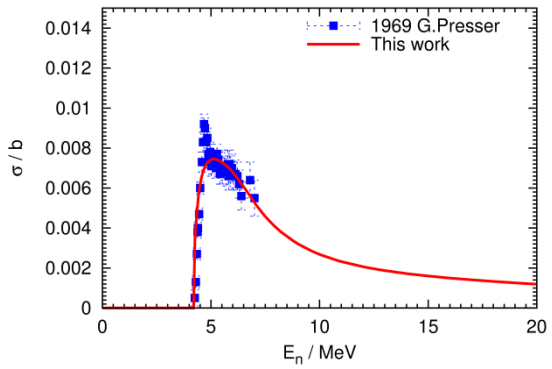

Fig. 6. The cross section of ^{6}Li(n,n$_2$) reaction.

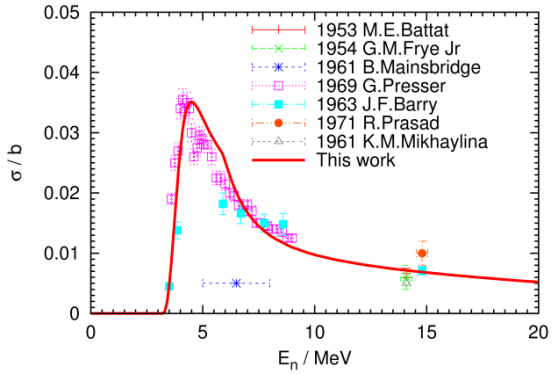

Fig. 7. The cross section of ^{6}Li(n,p) ^{6}He reaction.

The calculated result of ^{6}Li(n,p)^{6}He cross section is compared with the experimental data [22-28] in Fig 7.

Because the first excited state is unstable, the experimental data of (n,d) cross section should be the sum of ^{6}Li(n,n1) and ^{6}Li(n,d) cross sections. In Fig 8, the red curve is the sum of ^{6}Li(n,n1) and ^{6}Li(n,d) cross sections, the theoretical results are in good agreement with the experimental data [7, 10, 29, 30].

A fake channel of ^{6}Li(n,(2n))^{5}Li is defined to take place ^{6}Li(n,2n)^{5}Li channel. The calculated result shown in Fig. 9 is in agreement with the experimental data [28, 31, 32].

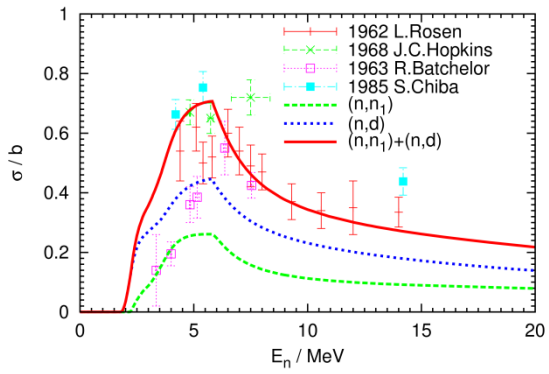

Fig. 8. The cross section of ^{6}Li(n,d) reaction.

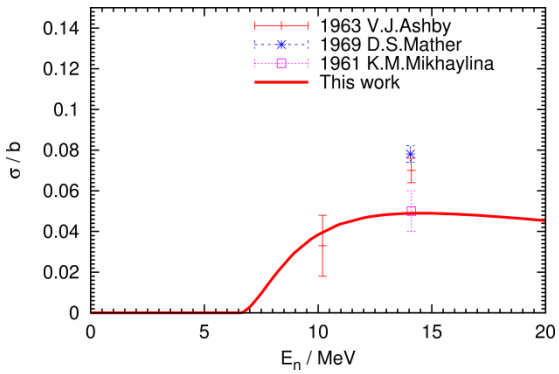

Fig. 9. The cross section of ^{6}Li(n,2n)^{5}Li reaction.

FDRR is developed for obtaining light nuclei cross sections and angular distributions. MLBW +reduced R-matrix method is used for analyzing n+^{6}Li reaction below 20MeV. Full matrix method is still under development. Preliminary result shows that full R-matrix method can improve the calculation results. In future, we will give different reduced resonance width for each state to further improve the calculation results. FDRR will be combined with LUNF [33] code and used for evaluations and updating CENDL.

References

[1] C.A. Goulding et al. Chicago Operations Office, A.E.C., Contract rept., **21**, No.3058, p.2 (1972) EXFOR 10252

[2] J.A. Harvey et al. Conf. on Nucl. Cross-Sect. and Techn., Washington 1975, **1**, 244 (1975) EXFOR 10451

[3] A.B. Smith et al. Nucl. Phys., A **373**, 305 (1982) EXFOR 10904

[4] H.H. Knitter et al. Euratom Reports, No.5726E, p.1 (1977) EXFOR 20749

[5] C.T. Hibdon et al. Nuclear Cross-Sections Techn. Conf., Washington, **1**,159 (1968) EXFOR 11163

[6] H.H. Hogue et al. Nucl. Sci. Eng., **69**, 22 (1979) EXFOR 10707

[7] J.C. Hopkins et al. Nucl. Phys., A **107**, 139 (1968) EXFOR 11153

[8] M. Drosg et al. Conf. on Nucl. Data f. Basic a. Appl. Sci. ,Santa Fe 1985, **1**, 145 (1985) EXFOR 12928

[9] H.H. Knitter et al. Euratom Reports, No.3454E (1967) EXFOR 20376

[10] S. Chiba et al. Jour. of Nucl. Sci. and Technology, **22**(10), 771 (1985) EXFOR 21986

[11] V.P. Alfimenkov et al. Yadernaya Fizika, **36**(5), 1089 (1982) EXFOR 40659

[12] C.M. Bartle. Nucl. Phys., A **330**, 1 (1979) EXFOR 10446

[13] C. Renner et al. Bulletin of the American Physical Society, **23**, 526(BI3) (1978) EXFOR 10841

[14] M.S. Coates et al. U.K. report to EANDC, No.151, p.10 (1973) EXFOR 20410

[15] D.B. Gayther. Priv. Comm: Gayther (1976) EXFOR 20862

[16] C.M. Bartle et al. Nucl. Phys., A **397**, 21 (1983) EXFOR 30651

[17] G. Zhang et al. Nucl. Sci. Eng., **153**, 41 (2006) EXFOR 32544

[18] P.W. Lisowski et al. Los Alamos Scientific Lab. Reports, No.8342 (1980) EXFOR 10854

[19] A.H. Armstrong et al. Nucl. Phys., **52**, 505 (1964) EXFOR 11024

[20] E.T. Sadowski et al. Bulletin of the American Physical Society, **27**, 624(C5) (1982) EXFOR 12900

[21] R. Batchelor et al. Nucl. Phys., **47**, 385 (1963) EXFOR 21147

[22] G. Presser et al. Nucl. Phys., A **131**, 679 (1969) EXFOR 21253

[23] M.E. Battat et al. Phys. Rev., **89**, 80 (1953) EXFOR 11058

[24] G.M. Frye, Jr.. Phys. Rev., **93**, 1086 (1954) EXFOR 11071

[25] B. Mainsbridge et al. Washington AEC Office Reports, No.1034, p.29 (1961) EXFOR 12660

[26] J.F. Barry. J. Nuclear Energy, Part A+B (Reactor Sci.Techn.), **17**, 273 (1963) EXFOR 22515

[27] R. Prasad et al. Nuovo Cimento A, **3**(3), 467 (1971) EXFOR 30336

[28] K.M. Mikhaylina et al. Neitronnaya Fizika, Moskva 1961, p.249 (1961) EXFOR 41226

[29] L. Rosen et al. Phys. Rev., **126**, 1150 (1962) EXFOR 11114

[30] R. Batchelor et al. Nucl. Phys., **47**, 385 (1963) EXFOR 21147

[31] V.J. Ashby et al. Phys. Rev., **129**, 1771 (1963) EXFOR 11119

[32] D.S. Mather et al. A.W.R.E. Aldermaston Reports, No.47/69 (1969) EXFOR 20794

[33] Jingshang Zhang. *Statistical theory of neutron induced light nucleus*. Science Press, 267-283. (2009)

New features on the digitization software GDgraph

Yongli Jin, Guochang Chen*, Jimin Wang

China Nuclear Data Center, China Institute of Atomic Energy, Beijing, 102413, China

Abstract. The evaluators and experimenters always desire to have full and latest experimental data sets. However, the data are often published as figures without numerical values for some publications or journals. Furthermore, the quality of figures is not always good enough, especially for some figures scanned from the hard copy of old publications. In the other hand, the researchers would like to retrieve the data directly from EXFOR database. Digitization of figures is only one method to obtain the numerical data and correlative uncertainty, when there are only figures available from publications. Therefore need a digitization software to fit the requirements from evaluation, measurement and EXFOR compilation in CNDC.

1. Introduction

GDgraph is a software for digitization. Since 1997, CNDC devotes to develop a software for digitization. The first version of digitization software GDGraph was developed and released in 2000 using VC++ language. Five years late, collected much feedback information on update and bugs of this software. The 2nd version of GDGraph software was released at 2006, in which the whole software was re-written using Perl computer language to obtain more comfortable conditions for programming and updating. The latest version 5.1 of GDGraph is released at 2016.

2. Main feature of GDGraph5.1

Some new features are developed since 2014 IAEA EXFOR Workshop.

(1) A shortcut as "Ctrl+Alt" is allowed to activate or deactivate the digitization point uncertainty from an image using "Arrows4Errors" function.

(2) It is possible to use "Tab" to assist the value setting for X-Y axis.

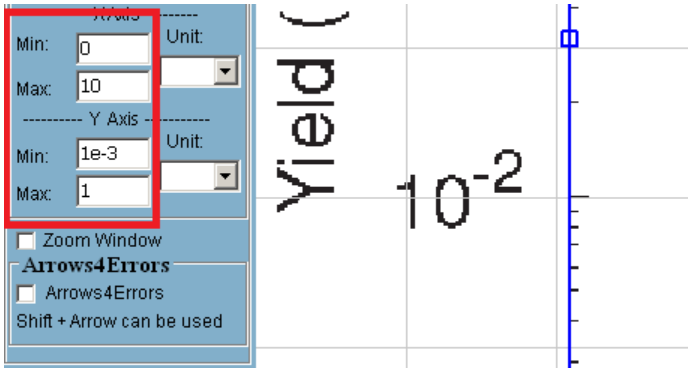

Fig. 1. Using "Tab" to assist the X-Y axis value setting.

(3) A new function is available for loading an image and resetting the original setting condition at "File" menu bar. There also provide a shortcut as "Ctrl+L" to realize this function. It will help user to start a new digitization work at the opening project.

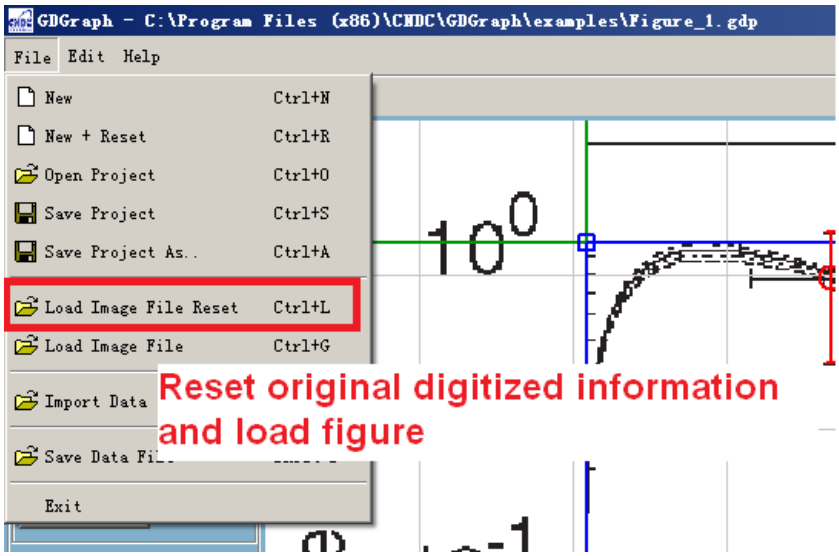

Fig. 2. "Load Image File Reset" allow to load an image and reset the original digitization setting.

(4) New option for output XY digitization data column order. Now there have two options as "x,dx+,dx-,y,dy+,dy-" and "x,y,dy+,dy-,dx+,dx-".

(5) The axis point could be activated or deactivated one by one using "Ctrl+x" or "Edit" at menu bar. Using magnifying glass function as "Zoom Window" to realize zoom-in axis point for digitzing XY axis in high quality. It is allowed to move the axis point by mouse or cursor keys. And the X-Y axes line color could be set using "Axis Color" in "Edit" menu bar to obtain high contract with the image.

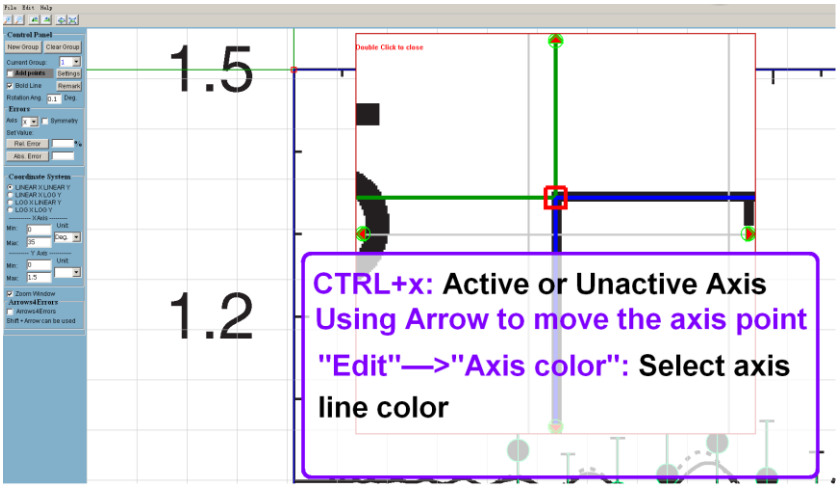

Fig. 3. A new function to assist XY axes digitization.

(6) Update the software to allow to show the actual digitizaton errorbar in Log data type in symmetry mode.

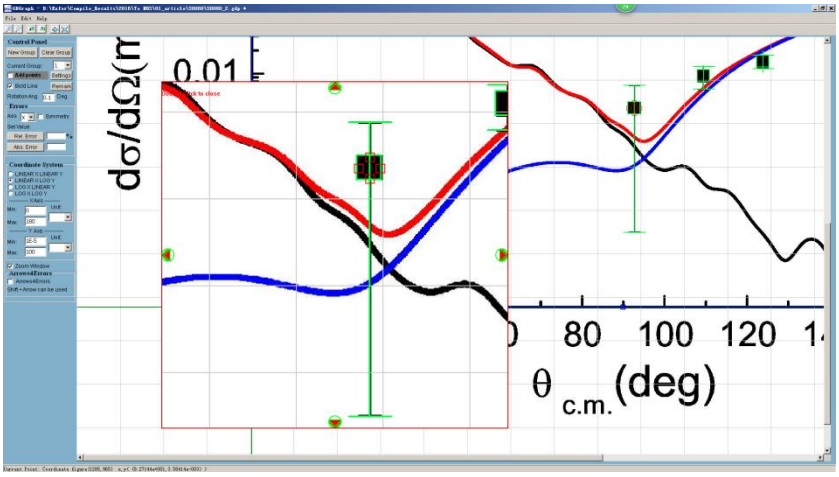

Fig. 4. Actually show the Log digitization data in symmetry mode.

4. Conclusion

Since 1997, the digitization software GDgraph is developed to fit the requirements of evaluation, measurement and EXFOR compilation. From the mold software to present version 5.1, GDgraph is mainly fit the requirements, although there are some aspects need to modify and add some new functions also.

Nuclear Data Section
International Atomic Energy Agency
P.O. Box 100
A-1400 Vienna
Austria

E-mail: nds.contact-point@iaea.org
Fax: (43-1) 26007
Telephone: (43-1) 2600 21725
Web: http://www-nds.iaea.org/